TAMPEREEN TEKNILLINEN YLIOPISTO
TAMPERE UNIVERSITY OF TECHNOLOGY

SONET MOLLICK

DESIGN AND IMPLEMENTATION OF MAXIMUM POWER POINT TRACKING ALGORITHMS FOR WIND ENERGY CONVERSION SYSTEMS

Master of Science Thesis

Examiners: Asst. prof. Paavo Rasilo
And Ph.D. Jenni Rekola
Examiners and topic were approved
on 28 February 2018

ABSTRACT

SONET MOLLICK: Design and implementation of maximum power point tracking algorithms for wind energy conversion systems
Tampere University of Technology
Master of Science Thesis, 64 pages, 1 Appendix page
May 2018
Master's Degree Program in Electrical Engineering
Major: Smart Grids
Examiners: Assistant professor Paavo Rasilo and Ph.D. Jenni Rekola

Keywords: Direct-drive, Maximum power point tracking (MPPT), Permanent magnet synchronous generator, Vector control, Wind energy conversion systems.

The thesis is carried out for the wind energy conversion development project at Laboratory of Electrical Energy Engineering of Tampere University of Technology. The main purpose of the thesis is to design four different types of maximum power point tracking algorithms (MPPT) in Matlab Simulink and analyze them based on their performance for the variable speed wind energy conversion systems. Since wind speed continuously varies in wind turbine systems, the MPPT algorithms are essential to maximize the energy yield from the wind at or under rated wind speed. Variable speed wind energy system can follow the wind speed variation and generate the maximum power under the normal operating condition at lower wind speed. The efficiency of the variable speed wind turbines relies on the performance of the maximum power point tracking techniques. However, for a specific wind speed there is only one available rotor speed which is responsible for maximum power yielding known as maximum power point (MPP). In the thesis all four MPPT scheme's theoretical backgrounds are explained and implemented in a simulation model. For all the control methods we need some input data such as wind speed, turbine characteristics, optimal power coefficient, and turbine power. In the tip speed ratio control method, precisely measured wind speed is required for the input of the MPPT controller and then the rotor speed reference is estimated from the given turbine characteristics and tip speed ratio. The simulation results show that it is the fastest control strategy to achieve the MPP but the accurate wind speed measurement is challenging. The optimal torque control and hill climb search control do not need any measurement of the wind speed but require measured turbine power. In the same manner, for the simulation of optimal torque control method, it is required to have the knowledge of optimal power coefficient which shows the optimal turbine power corresponding to the rotor speed. Eventually the most advanced method known as Modified hill climb search algorithm is simulated where turbine characteristics and wind speed measurements are not required. The thesis shows that every control method has their own pros and cons. For example, settling time for the optimal torque control and hill climb search control methods during the wind speed steps is about three times longer than with TSR control. Additionally, it is shown in simulation how the rotor speed fluctuation is eliminated with the help of Modified hill climb search algorithm. Finally, in the thesis a new concept called predictive MPPT is presented to improve the efficiency of the conventional MPPT algorithms.

PREFACE

This thesis work was carried out at the Tampere University of Technology for the wind energy development project between October 2017 and April 2018. At first, I would like to thank my supervisors Assistant Professor Paavo Rasilo and Ph.D. Jenni Rekola for the advice and help regarding my thesis. I wish to thank to my fellow partners Muhammad Ammar and Remy Farnert from TUT for helping me to understand the simulation concept. After all, thanks to Lauri, it was you who always gave me motivation and tried to push me to a new frontier.

Finally, I would like to thank my family and friends for all the support I have got throughout my studies.

Tampere, 28.2.2018

Sonet Mollick

CONTENTS

1. INTRODUCTION 1
2. THEORY 4
2.1 Wind energy conversion systems based on permanent magnet synchronous generator 4
2.1.1 Wind power theory 6
2.1.2 Mathematical modelling of Wind Turbine 7
2.1.3 Wind turbine simulation model 9
2.1.4 Mathematical and simulation model of PMSG 12
2.1.5 Steady state operation of wind turbine 15
2.1.6 Vector control of PMSG 16
2.2 Control strategy of PMSG 17
2.2.1 Constant torque region 18
2.2.2 Field weakening region 20
2.3 MPPT Control Techniques 20
2.3.1 Tip speed ratio control (TSR) 21
2.3.2 Optimal torque control (OTC) 22
2.3.3 Hill climb search control (HCS) 23
2.3.4 Modified hill climb search control 25
3. IMPLEMENTATION METHODS AND RESULTS 27
3.1 Tip speed ratio control 28
3.1.1 Simulation model 28
3.1.2 Simulation results 29
3.2 Optimal torque control 34
3.2.1 Simulation model 35
3.2.2 Simulation results 36
3.3 Hill climb search Control 41
3.3.1 Simulation model 42
3.3.2 Simulation results 43
3.4 Modified hill climb search control 49
3.4.1 Simulation model 51
3.4.2 Simulation results
4. CONCLUSIONS 59
REFERENCES 61
APPENDIX A 64

LIST OF ABBREVIATIONS AND SYMBOLS

AC	Alternating current
DC	Direct current
DFIG	Doubly fed induction generator
FW	Field weakening
HAWT	Horizontal axis wind turbine
HCS	Hill climb search
IGBT	Insulated gate bipolar transistor
MMF	Magneto motive force
MPP	Maximum power point
MPPT	Maximum power point tracking
MTPA	Maximum torque per ampere
MSC	Machine side converter
OTC	Optimal torque control
P&O	Perturb and observe
PI	Proportional integral controller
PMSG	Permanent magnet synchronous generator
PWM	Pulse width modulation
SCIG	Squirrel cage induction generator
TSR	Tip speed ratio
VAWT	Vertical axis wind turbine
WECS	Wind energy conversion systems
A	Area swept by the turbine blades (m^2)
$A_{threshold}$	Small power curve slope threshold $(\mathrm{Ws/rad})$
B	Damping coefficient
C_P	Power coefficient
d, q	Synchronous rotating reference frame variables
G	Gear ratio
I_s	Stator current (A)
I_{sm}	Maximum stator current of PMSG (A)
J	Inertia of the system (kgm^2)
K_m	Peak line to back e.m.f $(\mathrm{V/rpm})$
L_1	Line leakage inductance (H)

L_d	Synchronous d-axis inductance (H)
L_q	Synchronous q-axis inductance (H)
m_B	Mass of one blade (kg)
N_P	Number of pole pairs
p	Number of poles
P_e	Active electrical power (W)
P_{opt}	Optimal power point (W)
P_t	Actual electrical power produced by the wind turbine (W)
P_w	Mechanical power obtained from wind (W)
ΔP	Difference between present and previous power (W)
r	Turbine radius (m)
R_s	Stator winding resistance (Ω)
T_e	Generator electrical torque (Nm)
T_L	Turbine torque (Nm)
V_d	Stator d-axis terminal voltage (V)
V_{nom}	Rated wind speed (m/s)
V_{sm}	Maximum stator voltage of PMSG (V)
V_q	Stator q-axis terminal voltage (V)
V_w	Wind speed (m/s)
$W_{present}$	Present rotor speed (rad/s)
W_{last}	Previous rotor speed (rad/s)
α, β	Stationary reference frame variables
γ	Stator current angle (rad)
θ_e	Electrical rotor position (rad)
θ_m	Mechanical rotor position (rad)
λ	Tip speed ratio
λ_{opt}	Optimal tip speed ratio
ρ	Air density (kg/m^3)
ψ_{PM}	Flux linkage of permanent magnets (Wb)
ω_g	Generator rotor speed (rad/s)
ω_m	Turbine angular speed (rad/s)
ω_{ref}	Rotor reference speed (rad/s)

ω_{step}	Fixed step rotor speed reference $(\mathrm{rad/s})$
$\Delta\omega$	Rotor speed difference $(\mathrm{rad/s})$

1. INTRODUCTION

In recent years wind energy generation method is attracting great consideration due to its clean, pollution free, reliable features and growing realization of the negative impact of fossil fuel -based power generation. In the past couple of decades, wind turbines have turned out to be one of the most prominent strategies to produce renewable energy, demonstrated by the establishment of many Megawatt-turbines. However, the small wind turbines rated power up to 30 kW are less preferred. The issue of these turbines is the lower height of the nacelle, where the wind speed is less steady because of turbulences. Keeping in mind, the main goal is to increase the power yield during fluctuating wind situations, variable speed wind turbines are essential with a sufficient optimal power point tracking system [1].

The variable speed wind energy generating system is more profitable than the fixed speed generating systems in terms of production maximization, minimizing the flicker phenomena and aerodynamic performance below rated wind velocity [2] [3]. Variable speed wind energy systems can follow the wind speed variation and generate the maximum power under the normal operating condition at lower wind speed (speed lower than rated wind speed). When the wind speed becomes higher than the rated wind speed, the machine load control or the pitch angle control system takes the responsibilities to generate the constant power from the wind turbine [4]. The efficiency of the variable speed wind turbines relies on the performance of the maximum power point tracking (MPPT) techniques. However, for a certain wind speed, there is only one available rotor speed which is responsible for maximum power yielding known as maximum power point (MPP) [5]. In variable speed generating method for different wind velocities, the wind turbine can be driven at maximum power point by controlling the rotor speed optimally [3].

In wind energy conversion systems (WECS) different types of generator are used such as doubly fed induction generator, squirrel cage induction generator and permanent-magnet synchronous generator (PMSG) [5]. Among these PMSG are getting much attention in variable speed generation due to their better controllability, smaller size, higher energy density profile, less maintenance, direct driven minimizing the mechanical issues [6]. In order to achieve the optimal power operating point at or below the rated wind velocity, different types of MPPT algorithms are developed [2]. In this thesis four types of MPPT strategies and their simulated results will be analyzed based on the variable-speed generation system using a PMSG. All the control strategies have the objective is to control the generator speed to its optimal operating power point, depending on measurement of wind

speed, generator rotor speed, generator side current and voltage. In overall context of WECS the MPPT control strategies can be categorized into four classes known as tip speed ratio (TSR) control, optimal torque control (OTC) and hill climb search (HCS) control and modified hill climb search method [1] [7].

From a wind turbine systems, two parameters are accessible by estimation, i.e. pitch angle and wind speed comparing to the wind speed for appropriate operation. However, for small wind turbine system, the pitch angle is always kept fixed. According to the TSR control method, the turbine shaft speed is mainly adjusted to keep up the optimal tip speed ratio calculated utilizing measured wind and turbine shaft speed. Despite the fact that this technique is very simple and fastest MPP tracker, it depends profoundly on the precision of the wind speed measurement which is a big challenge for this strategy [6].

The concept of OTC technique is to modify the generator torque with respect to optimal reference torque of the wind turbine at a given wind speed. The concept of OTC technique is to modify the generator torque with respect to optimal reference torque of the wind turbine at a given wind speed. In this strategy the relationship is achieved by the optimal power coefficient. Because of an iterative procedure, the wind turbine will reach to its MPP [8]. Hill climb search is a perturb and observe (P&O) technique which observes the variation of the rotor speed and the generator power and decides either a positive or negative fixed step of rotor speed must be added to the earlier rotor speed reference corresponding to the power coefficient curve. The electrical power obtained from the machine side converters is used as an input in this method. This strategy does not need any prior knowledge of the turbine parameters, yet it is responsible for introducing hysteresis around the MPP. Finally, the fourth method modified hill climb search method is an improved MPPT system which is responsible for maintaining the rotor speed fixed at the MPP that includes a hill climber with variable step. It improves the tracking proficiency of the HCS method in which step size is scaled based on the slope of the power corresponding to the control variable (rotor speed).

The thesis objective is to investigate the performance of all types of MPPT algorithms with different wind speeds in detailed using Matlab Simulink software. The simulated results from the Simulink for different methods will be compared and analyzed based on their efficiency and complexity. Both fixed and variable wind speed will be applied to justify the efficiency of the algorithms and eventually new research areas will be proposed to develop the performance of the algorithms.

The thesis includes designing, simulating and testing the MPPT algorithms for both slow and sudden wind speed variation based on PMSG. The thesis is structured into several chapters. The construction and working principle of wind energy conversion system is explained in Chapter 2. Chapter 2 illustrates also the core concepts of PMSG control strategy and the basic principle of MPPT methods.

A description of the MPPT simulation model in Simulink along with results are presented in Chapter 3. Finally, Chapter 4 draws the conclusion. It comprises of reviewing the outcomes, comparative analysis of different MPPT methods to justify their effectiveness based on simulated results and possible future research work.

2. THEORY

This chapter presents the theory related to wind energy conversion system configuration. The goal of the system is to convert the kinetic energy contained in the wind into electrical energy using a generator. In the initial two subchapters, the hypothesis of the wind turbine with PMSG and its control strategy will be evaluated. The investigation in this thesis was limited to depict the theory of a wind turbine and synchronous generator. Finally, in the last section different MPPT algorithms will be presented.

2.1 Wind energy conversion systems based on permanent magnet synchronous generator

Since the early time of creating wind turbines, impressive endeavors have been made to use three-phase synchronous generators. It has the preferred standpoint that the field excitation can be adjusted, yet it creates complication of both machine and control part. Whenever the generator rotor is driven by the turbine, a three-phase power is induced in the armature windings of the generator which is transferred to the main utility grid through power converters and transformers. The PMSG has few elevated points of interest in WECS since they are steady and secure during the typical operation. Additionally, they do not require any extra DC supply for the field excitation which also makes the machine able to deliver active power [9]. In permanent magnet synchronous generator field winding (and its related power losses) is replaced by the pilot exciter (permanent magnet) for providing constant magnetic flux. This kind of machine can be built with the huge number of magnetic pole to lessen the synchronous mechanical speed. A cutaway diagram of a permanent magnet synchronous machine is shown in Figure 2.1. Because of its lower speeds, the machine is suitable to be driven directly by the turbine. As a consequence, it saves the cost of maintaining gear boxes which is responsible for most wind turbine failures. Because of its smooth control strategy, this type of machine is particularly suitable to use for variable speed operation with the help of a full rated power converter [1]. It is not possible to generate electric power of constant frequency with PMSG due to the variation of actual wind speeds. Therefore, PMSG ought to be associated with the utility grid through AC-DC-AC conversion systems by power converters.

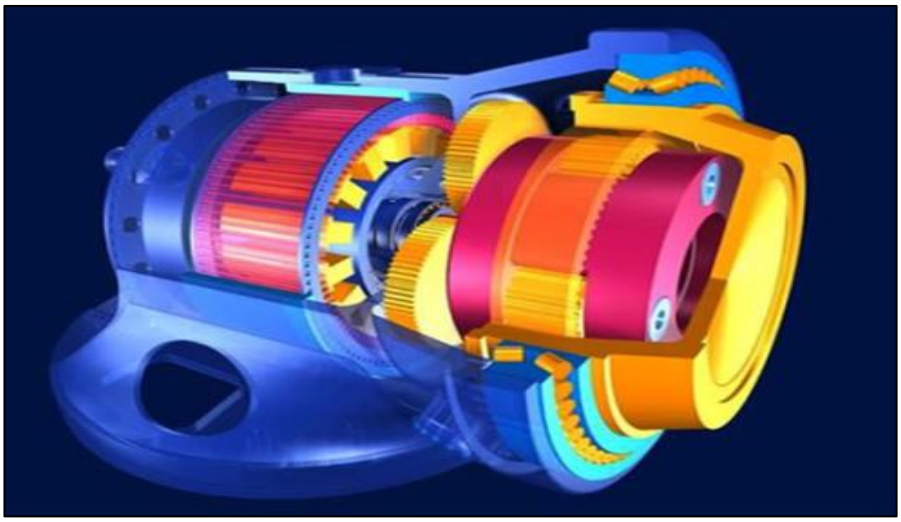

Figure 2.1 Cross section of a permanent magnet synchronous generator [10]

At first, the generated power with variable magnitude and frequency is converted into constant DC and afterward changed over again into AC power with settled magnitude and frequency through inverter. In Figure 2.2, the general construction of a wind turbine configuration is shown [11].

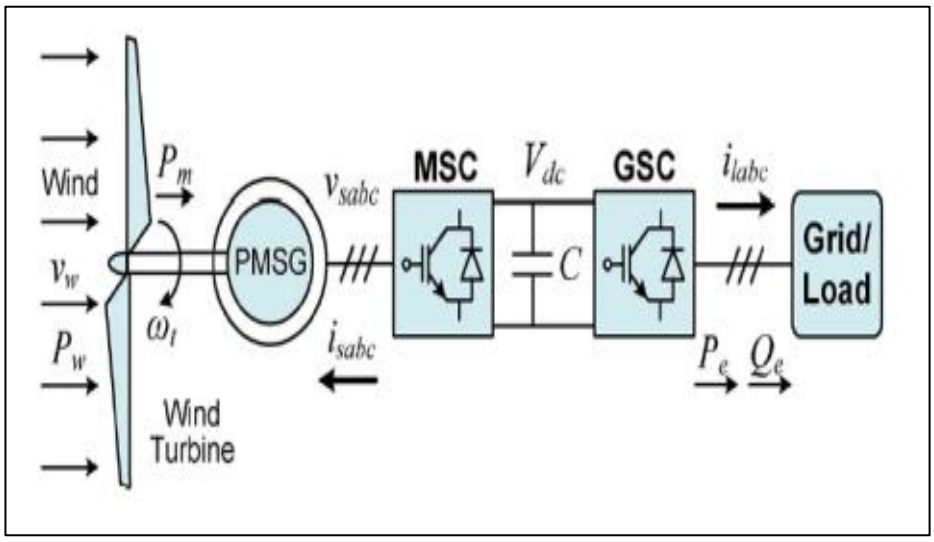

Figure 2.2 Schematic diagram of a direct-driven PMSG based wind generation system [11].

The whole system is a composition of machine side converter and a grid side converter interconnected by means of DC-link [11]. In invariable speed turbines, the converter is responsible for adjusting the shaft speed in capacity of the wind speed to drive the wind turbine constantly to its maximum operating point. Alongside the aerodynamic performance of the turbine, the rectifier is the fundamental segment that mainly decides the

efficiency of the entire system but it depends on what kind of MPPT method we are utilizing to maximize the power output. The generator efficiency is also being considered because it controls the armature currents [1].

2.1.1 Wind power theory

In Figure 2.3, the power obtained from a wind generator is shown corresponding to the different wind speeds. In the same manner, from the relationship between rotor speed and turbine torque can be manipulated as presented in the same figure. The figures prove that turbine torque and power are the functions of wind speed and the rotor speed. In Figure 2.3 all the MPPs are connected in the MPP curve at various wind speeds and it demonstrates that actually MPPs are not the maximum operating torque values rather than the optimal torque point. The stable operation of the generator is located on the right side of the torque characteristics curve where torque decreases corresponding to the generator speed. Since for a particular wind speed there is a maximum rotor speed beyond which the power curve goes to the negative side and the generation hypothetically stops. For the speed controlled wind energy systems, the generation will be stable if the commanded speed is less than the maximum speed. Basically, a speed loop is responsible to generate a torque command which is translated into a current command to the machine control system [6]. On the other hand, the generator torque should not be exceeded the maximum available torque from the wind. This way the system stability and continuous generation will be maintained.

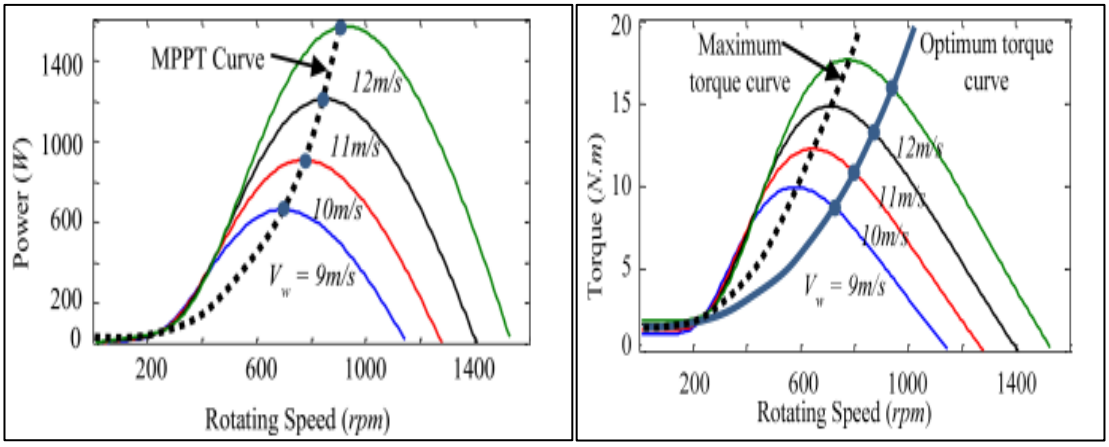

Figure 2.3 Turbine power characteristics with respect to shaft angular speed at different wind speeds (left). Turbine torque characteristics curve with respect to shaft angular speed at various wind speeds (right) [6].

2.1.2 **Mathematical modeling of Wind Turbine**

There are two types of wind turbines, vertical axis and horizontal axis turbine as shown in Figure 2.4. In terms of efficiency, the horizontal axis wind turbine (HAWT) is better than the vertical axis turbine (VAWT). The mechanical power contained in the wind turbine is defined with the following equation

$$\mathrm{P_w} = Av_w.\ \frac{1}{2}\rho v_w^2 = \frac{1}{2}\ \rho A v_w^3 \tag{2.1}$$

where $A = \pi r^2$ is the area swept by the turbine blades (r being the blade radius), ρ is the air density, and v_w is the wind speed [5]. Power coefficient C_p of a turbine is the ratio of the actual power transferred by the turbine and theoretical power available in the wind.

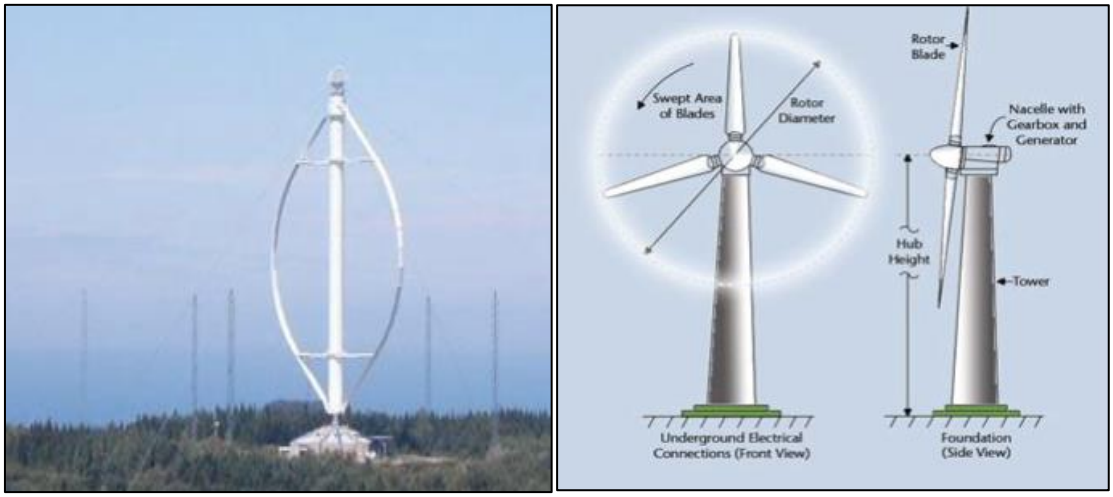

Figure 2.4 Two different types of wind turbine a) HAWT on left b) VAWT on right [12].

$$C_p = \frac{P_t}{P_w} = \frac{P_t}{\frac{1}{2}\rho A v_w^3} \tag{2.2}$$

C_p is the function of TSR which is defined by the λ and pitch angle (β) of the turbine blade and P_t, P_w are the actual electrical power produced by the wind turbine and theoretical power available flowing into the wind turbine blades respectively. In the thesis, the pitch angle is always kept constant for small wind turbine due to its mechanical complexity and expensive construction. Thus, the C_p is given by the following equation [13].

$$C_p(\lambda) = \left(\frac{116.46}{\lambda} - 10.53\right) e^{-18.4/\lambda} \tag{2.3}$$

In present days in many wind energy generation systems the maximum value of C_p is set at $C_{p,max}$ = 0.44. The tip speed ratio λ is the blade tip speed to the wind speed and it is given by the following equation

$$\lambda = \frac{r\omega_m}{v_w}, \tag{2.4}$$

where ω_m is the turbine angular speed. The power coefficient is a measure of the aerodynamic performance of the blades and it has a maximum value for a particular TSR. It's possible for a wind turbine to run only for a constrained range of wind speed. Underneath of a specific wind speed (cut-in speed v_{ci}), the turbine will not run due its static friction. It keeps the machine to remain in stand-still and then the value of λ will be zero. The system will generate electricity whenever the wind speed is above the cut-in speed. In order to run at its maximum power coefficient the turbine control system should figure out the optimal TSR (λ_{opt}). In the case of wind speed higher than the rated wind speed (v_{nom}), the turbine shaft speed will be kept in a small speed range to protect the rotor from damage and it is possible by controlling the pitch angle of the turbine. The turbine shaft will be running in its nominal rated speed (ω_{nom}). We obtain the maximum power coefficient ($C_{p,max}$) when the optimal tip speed ratio is 6.91. An example of a power coefficient curve is shown in Figure 2.5 [1].

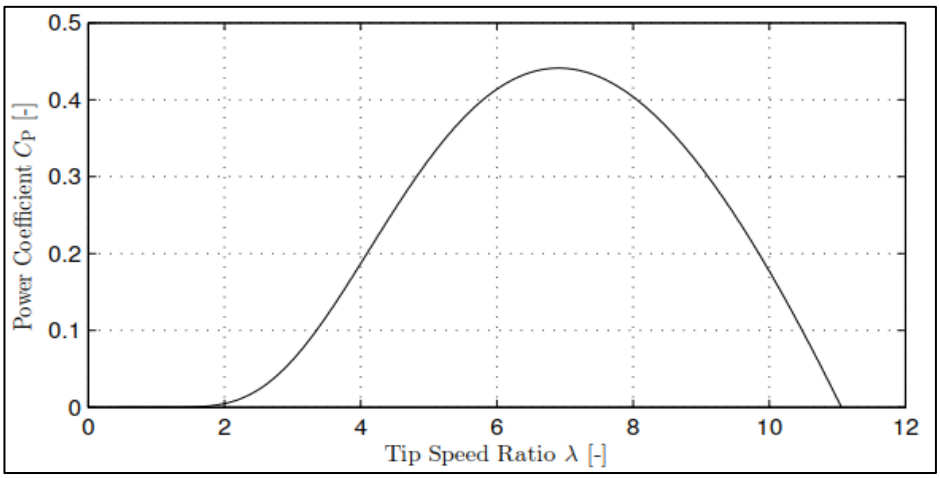

Figure 2.5 An example of relationship between TSR and power coefficient [1].

2.1.3 **Wind turbine simulation model**

The Simulink block diagram of a wind turbine is shown in Figures 2.6 and 2.7 respectively.

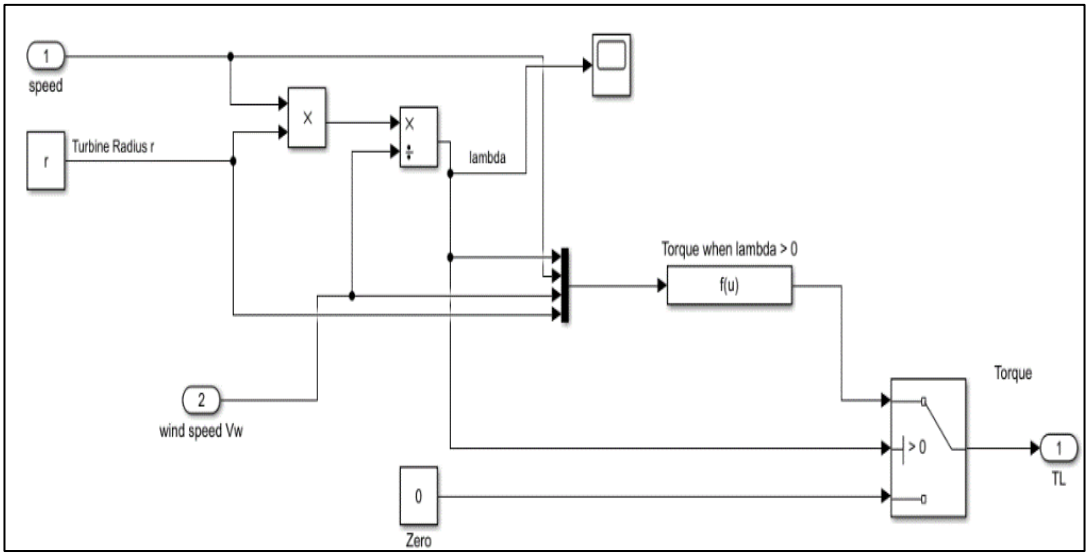

Figure 2.6 Simulink model of wind turbine torque $\boldsymbol{T_L}$.

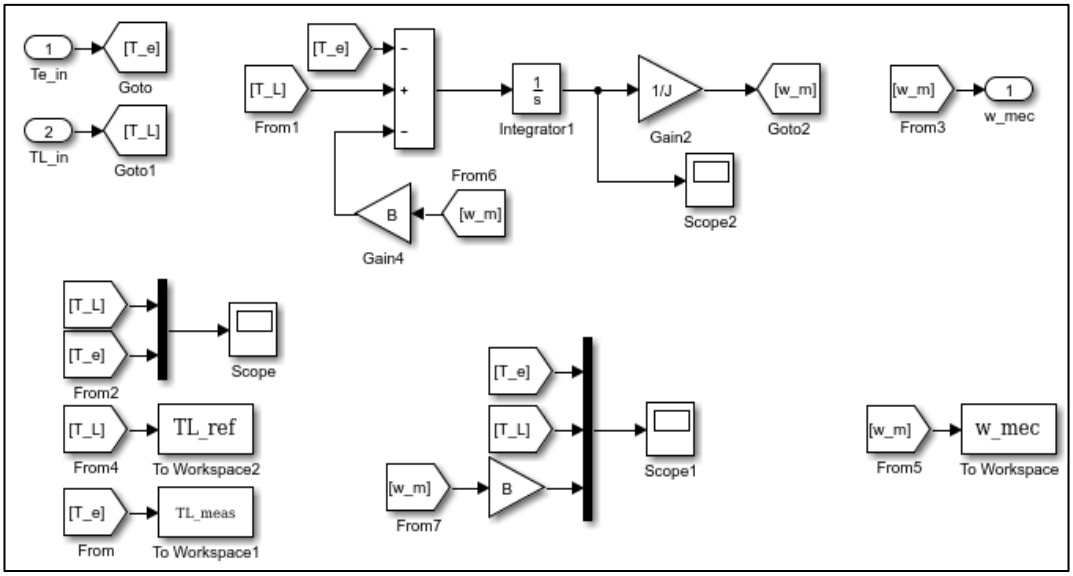

Figure 2.7 Simulink model of the angular speed of the turbine shaft.

The turbine system comprises of two major parts. The turbine torque (T_L) is calculated with the following equation

$$T_L = \frac{P_t}{\omega_m} = \frac{1}{2}\rho\pi r^2 \frac{C_p(\lambda)v_w^3}{\omega_m}. \quad (2.5)$$

The other part is responsible for modelling the mechanical system (generator + wind turbine). Additionally, the shaft speed is computed by means of generator electrical torque T_e and turbine mechanical torque T_L. The equation can be expressed with the swing equation

$$J\frac{d\omega_m}{dt} = T_L - T_e - B\omega_m, \tag{2.6}$$

where, J is the inertia of the mechanical system and B is the damping coefficient.

Equation (2.6) is called the equation of motion of wind energy conversion. When T_L is larger than $(T_e + B * \omega_m)$ that means the turbine-generator combination is accelerating and vice versa. The time taken by the turbine to achieve its MPP is mostly dependent on the total system inertia. The turbine model should be designed in such a manner so that its nominal power is fitted with generator nominal power. The machine parameter values that have been used in the thesis are attached in appendix A. These machines could be used in the wind turbine laboratory prototype. Both of machines are rated to 30 kW in delta connection at 370 V, but they can be used in star connection rated with 17 kW with the same terminal voltage.

Now the estimation of wind-turbine parameters for 17 kW PMSG is done in the Table 2.1. The aim of this task is to obtain reasonable dimensions for a hypothetical wind turbine, which could be used to supply the 17 kW PMSG in the laboratory prototype. Our goal here is to scale two turbines with appropriate gear ratio and inertia corresponding to the 17 kW PMSG. Now the theoretical power contained in the wind is given by equation (2.1).

The maximum power coefficient given by equation (2.7) is $C_{p,max}$ = 0.44 at $\lambda = \lambda_{opt}$ = 6.91. Using these constant values, we can obtain the following parameter i.e. maximum turbine power and mechanical speed.

$$P_w = \frac{1}{2}\rho A\, C_{p,max} v_w^3 \tag{2.7}$$

$$\omega_m = v_w \frac{\lambda}{r} \tag{2.8}$$

Thus, the turbine radius and speed can be scaled from size 1 to size 2 as

$$r_2 = \left(\sqrt{\frac{P_{w,2}}{P_{w,1}}}\right) r_1 \tag{2.9}$$

$$\omega_{m,2} = \frac{r_1}{r_2}\, \omega_{m,1} \tag{2.10}$$

It is accepted to be assumed that the volume of a turbine blade is proportional to cubic power of wind turbine size. The inertia can be obtained as

$$J = \frac{1}{3} m_B r^2 \tag{2.11}$$

where m_B is the mass of one blade.

In the same way, the moment of inertia J of the turbine can be scaled as

$$J_2 = \left(\frac{r_2}{r_1}\right)^5 J_1 \tag{2.12}$$

In the lab prototype setup, $P_{w,2} = 17$ kW and we want to find reasonable turbine radius r_2, mechanical speed $\omega_{m,2}$ and moment of inertia J_2 based on equations from (2.9) to (2.12). The generator rated speed is 13.3 rad/s which is corresponding to 127 rpm. Thus, a gear with a gear ratio G may need to be used which is expressed with the following equation

$$G = \frac{\omega_G}{\omega_{m,2}}, \tag{2.13}$$

where ω_G is the generator rated speed [13]. We used two different types of parameters value mentioned in the Table 2.1. In the second case the inertia or the mass of the blades is not reported.

Table 2.1 Parameter values for scaling two turbines to 17 kW.

Case 1				**Case 2**			
r_1	1.27 m	r_2	5.24 m	r_1	69.3 m	r_2	5.09 m
$P_{w,1}$	1 kW	$P_{w,2}$		$P_{w,1}$	3150 kW		
$\omega_{m,1}$	49.22 rad/s	$\omega_{m,2}$	11.94 rad/s	$\omega_{m,1}$	1.12 rad/s	$\omega_{m,2}$	14.25 rad/s
m_T	7 kg	G	1.11			G	0.93
J_1	1.25 kgm^2	J_2	1495 kgm^2			J_2	1495 kgm^2

From the calculation based on the parameters of the Table 2.1, we see that for both of cases the gear ratio is close to 1. Thus, we can set the generator speed and the turbine

mechanical speed 13.3 rad/s for both cases. It is possible to estimate the angular speed of the rotor utilizing the mechanical speed sensor or with the help of numerical calculation (sensor less scheme) utilizing with this expressed equation

$$\omega_m = \frac{(V_{dc}+2R_s i_L)}{\frac{3\sqrt{3}K_m}{\pi} - \frac{p(L_1+L_s)i_L}{20}} \tag{2.14}$$

where ω_m is the measured mechanical rotor speed, R_s is the stator resistance, L_s presents stator inductance, L_1 is the in line leakage inductance, p is the number of poles of the machine, K_m depicts the constant term of peak line to back emf [14]. In reality wind speed fluctuates instantaneously so therefore it is always efficient and cost effective to develop such a speed sensor less scheme to implement with the MPPT control system. The results from the above two cases are close to each other. Based on the calculations, reasonable turbine parameters corresponding to our lab setup could be the following: Blade radius $r = 5.2$ m, rotation speed $\omega_m = 13.3$ rad/s (corresponding to 127 rpm), gear ratio $G = 1$ (direct drive configuration), moment of inertia $J = 1495$ kgm^2.

2.1.4 **Mathematical and simulation model of PMSG**

We can express the stator voltages of the permanent magnet generator in synchronous reference frame. The frame is stationary in comparison with the generator rotor, and it comprises of quadrature (q) and direct (d) axes. The d-axis of the machine is located along the rotor winding. The q-axis lags 90 electrical degrees of the d-axis. To find out the synchronous reference frame, first three-phase variables (a, b, c) must be transformed into a fixed stator reference frame to (α, β)-components using Clarke's transformation with the following equations

$$V_\alpha = \frac{2}{3}(V_a - \frac{1}{2}V_b - \frac{1}{2}V_c) \tag{2.15}$$

$$V_\beta = \frac{1}{\sqrt{3}}(V_b - V_c). \tag{2.16}$$

It is required to know the electric angle θ, the angle between the a-phase and q-axis, to transform the (α, β) reference framework into the synchronous reference (d, q) coordinate system. It is estimated with the help of using the rotor mechanical angle θ_m and the pole pair number N_p of the machine.

$$\theta = N_p\theta_m \tag{2.17}$$

Next, the (α, β) -components are converted to (d, q) -components by means of the Park's transformation

$$V_q = V_\alpha cos\theta + V_\beta sin\theta \tag{2.18}$$

$$V_d = -V_\alpha sin\theta + V_\beta cos\theta, \tag{2.19}$$

where V_d and V_q are the d- and q-axis stator voltages respectively. The same transformation can be made for stator currents and stator fluxes as well.

In Figure 2.8 the different types of voltage components are drawn schematically in three different reference frameworks.

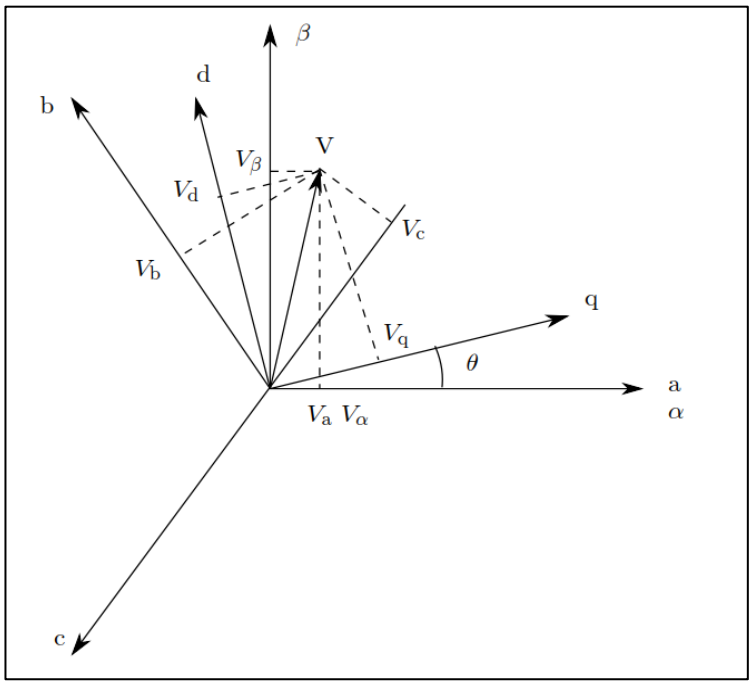

Figure 2.8 The voltage components in stator and synchronous reference frame [1].

Finally, we can derive the PMSG voltage equations for the stator in synchronous reference frame as

$$V_q = -R_s I_q - L_q \frac{dI_q}{dt} + \omega_e \psi_{PM} - \omega_e L_d I_d \tag{2.20}$$

$$V_d = -R_s I_d - L_d \frac{dI_d}{dt} + \omega_e L_q I_q, \tag{2.21}$$

where R_s is stator resistance, ω_e is the rotational electrical speed, ψ_{PM} is the permanent magnet flux linkage, L_d,L_q are the stator equivalent inductances in d- and q- axes respectively. Electrical speed can be written by rate of change of angular position as follows

$$\omega_e = \frac{d\theta}{dt}. \tag{2.22}$$

The equivalent circuit diagrams of the (*d, q*) coordinate system are drawn schematically in Figure 2.9. The decoupling term, the inductance and induced EMF in the q-axis equivalent circuit can be seen in the figure.

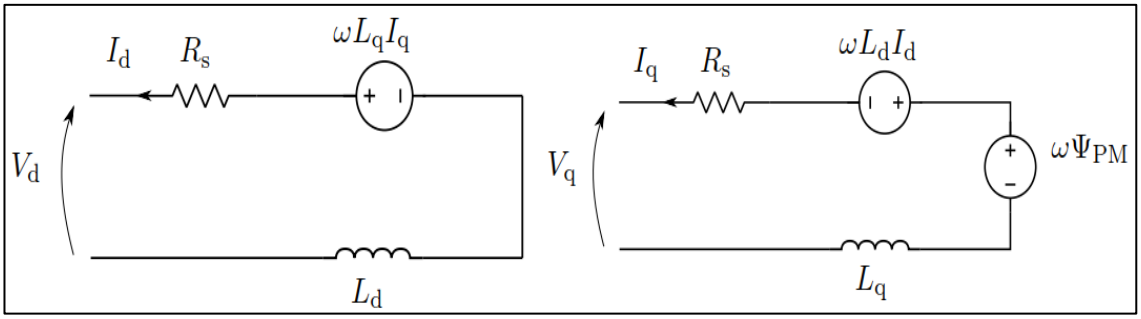

Figure 2.9 On left d-axis equivalent circuit, on right q-axis equivalent circuit [1].

In synchronous reference frame, the induced electrical power P_e can be written in terms of stator d-and q-axis voltages and currents as follows

$$P_e = \frac{3}{2}\,(V_d\, I_d + V_q\, I_q). \tag{2.23}$$

Next, we can substitute the equations (2.20) and (2.21) into (2.23) which gives

$$P_e = \frac{3}{2}\, R_s\left(I_d^2 + I_q^2\right) + \frac{3}{2}\left(L_q\, \frac{d}{dt}\left(\frac{I_q^2}{2}\right) + L_d \frac{d}{dt}\left(\frac{I_d^2}{2}\right)\right) + \frac{3}{2}\left(\omega_e\, \psi_{PM}\, I_q + \omega_e\left(L_d - L_q\right) I_d I_q\right). \tag{2.24}$$

The first term in the equation (2.24) is the resistive losses in the machine, the second term is the difference of energy conserved to the magnetic field and the last one provides the developed electromagnetic power. The total produced electrical power to the grid can be defined as

$$P_e = \frac{3}{2}\left(\omega_e \psi_{PM}\, I_q + \omega_e\left(L_d - L_q\right) I_d I_q\right). \tag{2.25}$$

The electrical rotational speed can be transformed into mechanical speed with the following equation

$$\omega_e = N_p \omega_m. \tag{2.26}$$

The final derived equation for the electrical torque is

$$T_e = \frac{P_e}{\omega_m} = \frac{3}{2} N_p\left(\psi_{PM} I_q + \left(L_d - L_q\right) I_d I_q\right). \quad (2.27)$$

The first term in the equation (2.27) indicates the magnetic torque and the last term is known as reluctance torque [1] [15]. In the case of surface mounted PMSG, the reluctance term is absent. We can control the electrical torque mainly by controlling the I_q current component. This control method is used in the MPPT control strategies. A complete simulation block diagram of a PMSG is presented in Figure 2.10.

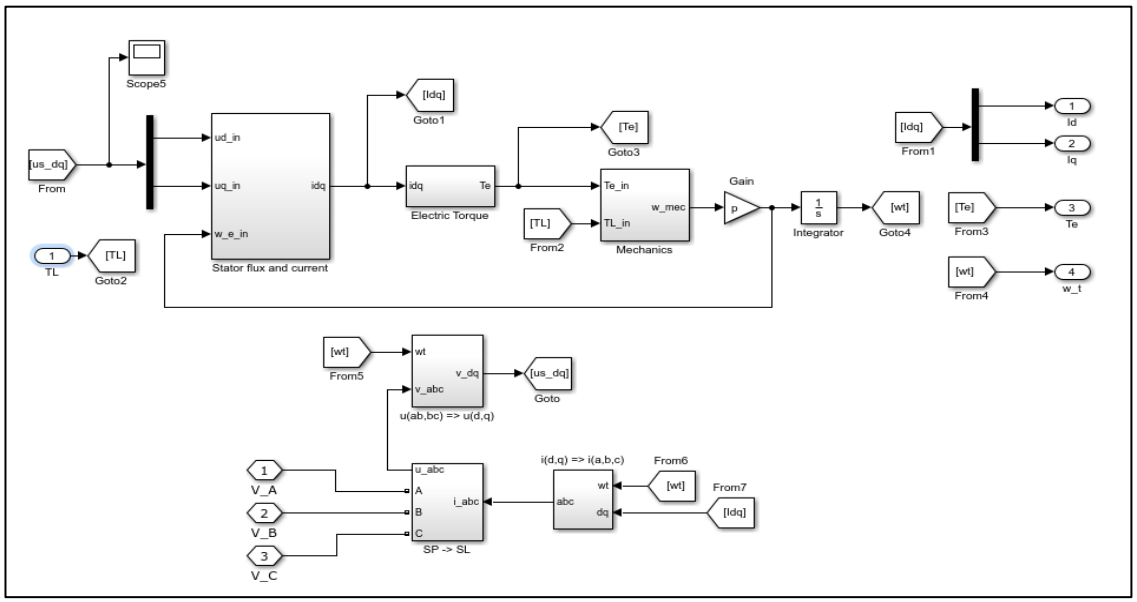

Figure 2.10 Complete Simulink model of the PMSG.

The model consists of three major subsystems i.e. stator flux and current, electric torque and mechanics. The three-phase currents (*a, b, c*) are transformed into two component synchronous reference frame (*d, q*) using the Clarke-Park transformation. In appendix A the PMSG parameters value are given for simulation.

2.1.5 **Steady state operation of wind turbine**

Based on the available wind speed a variable speed wind generation system can be thought in working under two operational zones called lower wind speed operational and higher wind speed operational zone. One speed reference can be used for the mentioned two zones such as 10 m/s as wind speed reference and a maximum wind speed value for the simulation. The point between two operational zones is the nominal speed of the generator. Every point which is higher than the wind speed reference is considered to be in the higher speed zone. When the wind speed crosses the maximum speed reference value, the produced power from the turbine will be constant and the turbine rotational speed as well (see example Figure 2.11).

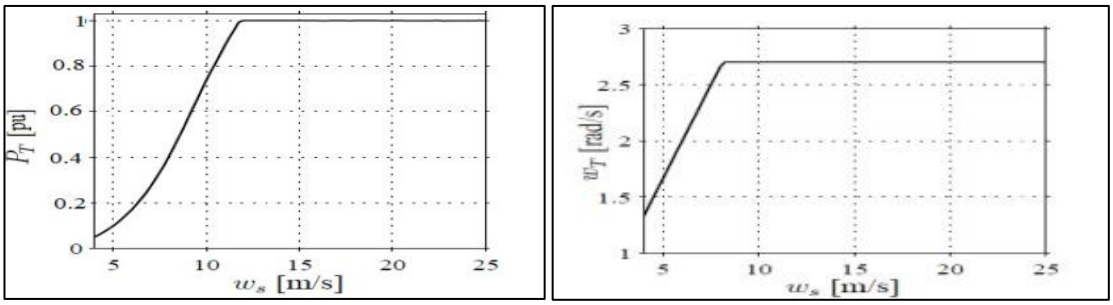

Figure 2.11 Relationship between power ($\boldsymbol{P_T}$) and wind speed ($\boldsymbol{\omega_s}$) (left) and relation between rotor rotational speed ($\boldsymbol{\omega_T}$) and wind speed ($\boldsymbol{\omega_s}$) (right) [14].

In the case of low wind speed operational zone, the tip speed ratio is in its optimum value by controlling the rotor speed. But when the maximum rotor speed and optimal (nominal) power is obtained, the rotor shaft speed is kept in its optimal (nominal) value. Every point which is lower than the reference wind speed value go to control zone. When the optimal power is achieved the pitch angle of the blades is kept constant to maintain turbine power to its optimal value [14].

2.1.6 **Vector control of PMSG**

The vector control is comprised of the controlling the three phase stator currents in dq-rotating reference frame. The schematic control block diagram is shown in Figure 2.12. The method is projection based which is transforming a three-phase speed and time dependent system into DC valued co-ordinate (d and q- components) system. In order to control the machines, two constants are required at the input side as references i.e. the stator flux and torque component. The flux component is aligned with the d-component and the torque component is aligned with the q component [16]. By the vector control (Field oriented control) it is possible to control independently the electromagnetic torque and stator flux linkage. In Figure 2.12 the variables with ‘‘*’’ (star) marked denote the reference value and the measured values are denoted without star marked. The output value of the machine is the rotational speed which is compared with the speed reference. Next, the PI type speed controller receives the error signal and generates the reference i_q^* current. On the other hand, the i_d^* reference current is estimated depending on control schemes of PMSG i.e. constant torque region and field weakening region. Two PI type current controllers with appropriate parameters will receive the reference i_d^* and i_q^* current subtracted from the i_d and i_q currents. The generated output of the both controllers is u_d^* and u_q^* voltage references respectively. To gain the decoupled control of dq-axes, it is needed to add or subtract the decoupling terms with the u_d^* and u_q^* voltage references. The dq-components later transformed to three-phase variables using the inverse Park transformation.

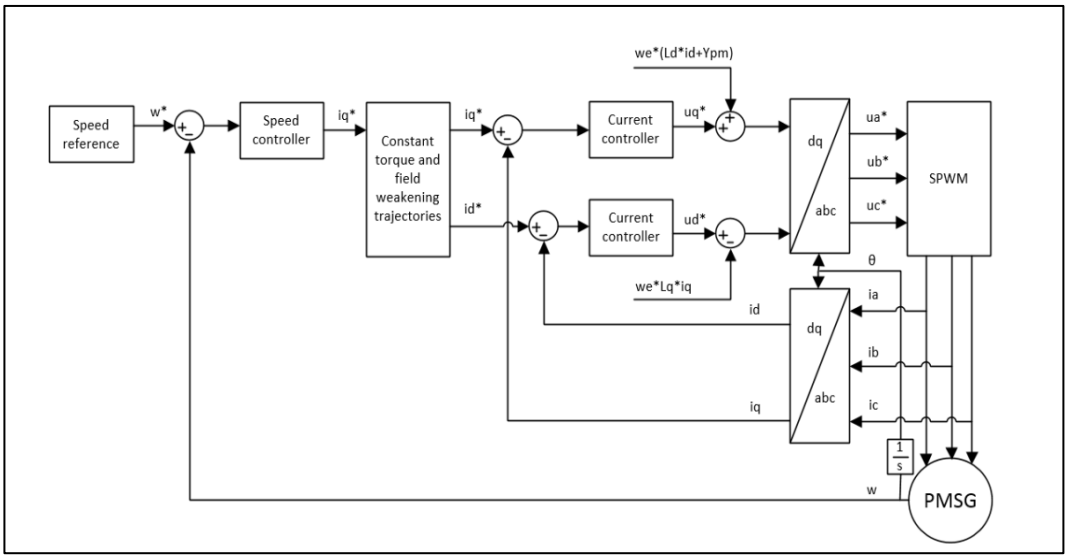

Figure 2.12 The vector control block diagram for PMSG [16].

The three phase variables are transferred to the pulse width modulation (PWM) block to generate the control pulse for the IGBTs. The estimated stator currents (*a, b, c* components) will be transformed to the *dq*- components with the help of Park's transformation. The transformation block requires the instantaneous rotor angular position in every time. The rotor angular position is obtained from the integration of rotor angular speed [17].

2.2 Control strategy of PMSG

In this chapter the control strategies of PMSG will be demonstrated briefly. We will mainly give focus on the vector control of the PMSG because in simulation the PMSG is assumed to be controlled by means of this control technique. In the first sub chapter we will discuss about two different types control techniques of PMSG i.e. constant torque region and field weakening region will be illustrated. Control strategy of permanent magnet synchronous machine is important to reduce the stator current losses and getting a wide speed range. Our goal is to maximize the output of the wind generation system in every aspect such as increasing the efficiency in terms of selecting the best MPPT algorithm and reducing the generator power loss. Therefore, proper control strategy of the synchronous machine is inevitable to apply for reducing the loss. It is possible with the help of maximum torque per ampere (MTPA) control method for the low speeds as well as field weakening technique in high speeds. Therefore, the control schemes can be classified into two categories based on nominal speed of the machine (Figure 2.13). In constant torque region the machine torque is maximum until the speed becomes nominal. In this time voltage and power increase linearly with respect to the speed. Then again when the speed is above the rated value, the generator will follow the constant power region characteristics. Here machine torque starts to decrease inversely corresponding to the speed, but power and voltage are kept constant [17].

2.2.1 Constant torque region

The stator terminal currents are reduced using the MTPA control method in the constant torque region. Thus, the power losses of the synchronous machine can be reduced. Equation (2.28) provides the maximum value of the electrical torque. We can calculate the nominal value of the stator current (I_s) angle in polar form:

$$I_s \angle\gamma = I_s\, cos(\gamma) + jI_s\, sin(\gamma) = I_{sd} + jI_{sq} \tag{2.28}$$

In which γ is the stator current angle. We can substitute the current equation obtained from the equation (2.29) in equation (2.28) with the magnitude and angle. Next the second- degree equation is partially differentiated for the stator current angle and putting the zero value on right side.

$$\frac{\delta T}{\delta \gamma} = \frac{3P}{2}\psi_{PM}\, I_s\, sin(\gamma) + \frac{3P\left(L_{sd}-L_{sq}\right)I_s^2\, sin(2\gamma)}{4} = 0 \tag{2.29}$$

The total torque of the machine is divided into magnetic and reluctance term. The Figure 2.13(b) shows both the magnetic and reluctance terms corresponding to the various stator current angles. We can see the optimum value of magnetic torque happen when the current angle is 90^0 and for the optimum reluctance torque the angle is 135^0.

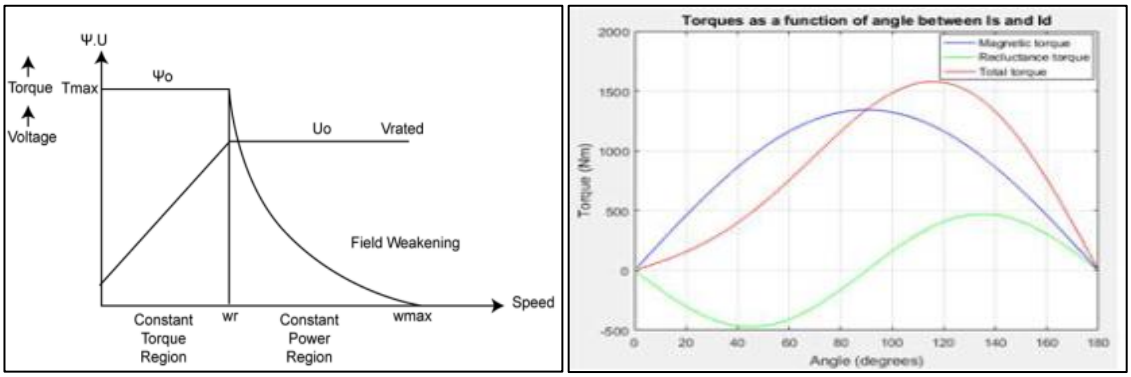

Figure 2.13 a) Constant torque and field weakening region with respect to speed b) different maximum torques respect to current angle [17].

First, we can determine the first arbitrary value of current I_{sq} component from the speed controller. After the determination of I_{sq} current, the following equation can be used to estimate the stator current component I_{sd}. The partial derivative of equation (2.30) we can use the stator current component in *dq*-components.

$$I_{sd} = \frac{\psi_{PM}}{2(L_{sq}-L_{sd})} - \sqrt{\frac{\psi_{PM}^2}{4\left(L_{sq}-L_{sd}\right)^2} + i_{sq}^2} \tag{2.30}$$

The current components I_{sd} and I_{sq} will not be in arbitrary. These are called the maximum value of the PMSG but there are constraints which are introduced by following

$$I_s = \sqrt{I_{sd}^2 + I_{sq}^2} \leq I_{sm} \tag{2.31}$$

$$V_s = \sqrt{V_{sd}^2 + V_{sq}^2} \leq V_{sm}, \tag{2.32}$$

where V_{sm} and I_{sm} are the maximum voltage and current of the PMSG respectively. V_{sm} is constrained by the DC- link voltage. In Figure 2.14 voltage and current constraints are shown in *dq*-complex plane.

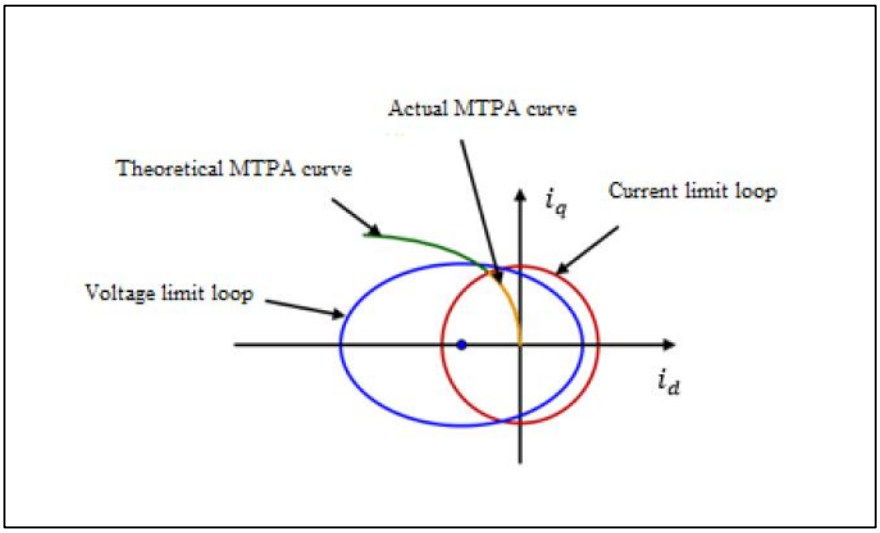

Figure 2.14 The voltage and current constraints with optimal MTPA Curve [17].

The current limit loop is in static shape since the maximum allowed stator current is constant. Then again, the voltage limit loop is in elliptical shape for various rotational speed of machine. The actual MTPA curve resides in the current limits and this should be followed when the machine is operated with low angular speed. The following equations estimate the maximum allowed current limit in d and q components

$$I_{smd} = \frac{\psi_{PM}}{4(L_{sd}-L_{sq})} + \sqrt{\frac{\psi_{PM}^2}{16(L_{sd}-L_{sq})^2} + \frac{I_{sm}^2}{2}} \tag{2.33}$$

$$I_{smq} = \sqrt{I_{sm}^2 - I_{smd}^2} \tag{2.34}$$

where I_{smd} is the maximum current in d component and I_{smq} denotes the maximum current in q component.

2.2.2 Field weakening region

The operating principle of a PMSG in field weakening region is more complex than the control in constant torque region. The induced back-EMF is proportional to the rotor speed and air gap field of the machine. It is possible to achieve wide constant power speed range for the PMSG. When the back-EMF ends up noticeably bigger than the maximum allowed output voltage then the PMSG will be unable to draw currents as well as producing torque. Therefore, the motor speed cannot be increased when the back-EMF crosses the threshold voltage unless the air gap flux is reduced. The magnetic field produced by the permanent magnet can be weakened with the help of stator MMF (magneto motive force) demagnetization. Thus, the speed range also can be increased noticeably. While the machine is operated in the field weakening (FW) region a demagnetizing MMF is created by the stator winding against the magnetic field of PM [18]. In the FW region the voltage limits are inversely proportional to the rotational speed of rotor. The Figure 2.14 indicates that flux weakening curve co-insides with the voltage limit loop. The concept of the FW control is to keep the stator voltage constant in its maximum value. The speed controller provides the current component i_{sq} as an output. The air gap flux is reduced with varying the current component i_{sd}. Thus, the rotor angular speed can be increased keeping the stator voltage stable. The stator terminal voltage can be written by the following way:

$$\frac{V_{sm}}{\omega_e} \geq \sqrt{\left(L_{sd}i_{sd} + \psi_{PM}\right)^2 + \left(L_{sq}i_{sq}\right)^2} \tag{2.35}$$

The component i_{sd} can be solved from equation (2.36) forming a second-order equation

$$i_{sd} = -\frac{\psi_{PM}}{L_{sd}} + \frac{1}{L_{sd}}\sqrt{\frac{V_{om}^2}{\omega_e^2} - \left(L_{sq}i_{sq}\right)^2} \tag{2.36}$$

where $V_{om} = V_{sm} - R_s I_{sm}$ when stator resistances are not accounted for. There would be a chance for current saturation at high speeds when the air gap flux is decreased using component i_{sd}. The d-axis current constraint i_{smd} can be written by the following way:

$$I_{smd} = -\frac{\psi_{PM}L_{sd}}{a} + \frac{1}{a}\sqrt{\psi_{PM}^2 L_{sd}^2 - ab} \tag{2.37}$$

In which $a = L_{sd}^2 - L_{sq}^2$ and $b = I_{sm}^2 L_{sq}^2 + \psi_{PM}^2 - \frac{V_{sm}^2}{\omega_e^2}$.

2.3 MPPT control techniques

In this chapter different MPPT control methods will be explained in detailed and how the wind turbine is controlled to its maximum power point based on the systems parameters

such as wind speed variation, rotor speed and generated power. The more estimations a technique needs, the more hardware needs to be installed. Therefore, the system complexity and cost are increased as well. Furthermore, the precise calculation of wind speeds is challenging therefore, there are different MPPT algorithms to compute the wind speed based on the other measurement parameters which are easy to estimate. For example, the DC-link voltage slope indicates the information of wind speed change and the acceleration of the rotor. The wind speed can be estimated as well by means of electric power output of the generator considering the systems dynamics and losses and then the calculated wind speed can be utilized to implement in the MPPT algorithm.

The safety features are provided also with the help of MPPT controller. For instance, while the wind speed is below the cut-in speed, the speed controller will halt the turbine to protect it from additional friction of the equipment. On the other hand, when the wind speed is higher than the rated wind speed, then the rectifier will be responsible to keep the turbine speed fixed to its rated value. But when the wind speed exceeds the cut-out speed, the turbine will be stopped to make the system safe from the damage.

The most used MPPT techniques are demonstrated below based on their effectiveness, simplicity features and control algorithms. The first two methods described in here i.e. tip speed ratio control and optimal torque control based on the mechanical parameters (torque, inertia, speed) of the systems and finally the hill climb search control and modified hill climb search control are based on the electrical quantities such as power (voltage and current) obtained from the rectifier.

2.3.1 Tip speed ratio control (TSR)

This is a direct strategy to execute since only the measured wind speed is required for the input of the MPPT controller. After that the reference rotor speed is estimated for the speed controller with the information of optimal tip speed ratio (λ_{opt}) and the radius of the turbine. It is possible to determine the optimal TSR theoretically or experimentally and can be saved as the reference [8]. The goal is to keep the TSR at its optimal value by measuring the turbine speed and instantaneous wind speed. Basically, a typical well-tuned PI type speed controller appropriate parameter values is required for controlling optimal rotor speed [19]. In the thesis the speed controller was designed with the Ziegler-Nichols method for both constant and variable wind speed condition.

$$\omega_{ref} = \frac{v_w \lambda_{opt}}{r} \tag{2.38}$$

where ω_{ref} is reference rotor speed, r is the turbine radius and λ_{opt} is the optimal tip speed ratio. In our case the value of the optimal TSR is 6.91 and it can be seen from the $C_P(\lambda)$ curve (see Figure 2.5). A basic block diagram of tip speed ratio control is presented

in Figure 2.15 for better understanding. In the figure ω_g depicts as the generator rotor speed. This is the simplest and fastest MPPT method because it gives the precise location of the MPP. For the proper tracking of the MPP, system's characteristics data such as turbine's blade model and generator parameters should be obtained in advance.

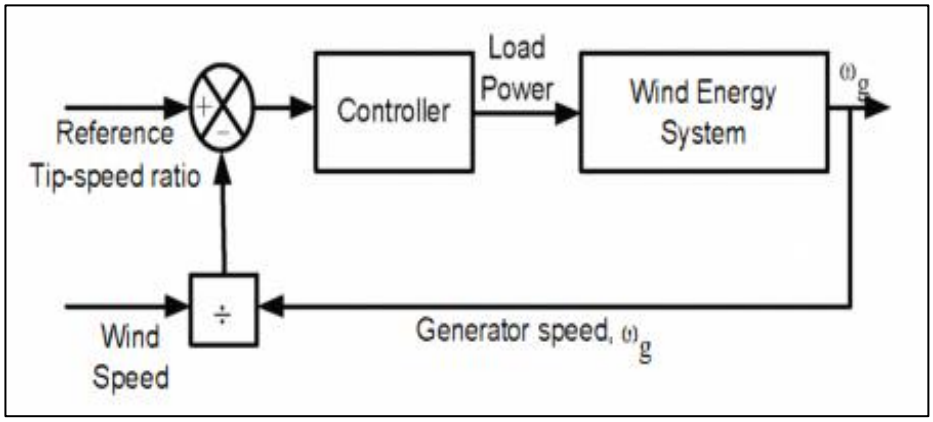

Figure 2.15 Schematic block diagram of TSR control [8].

The wind speed sensor is needed for the accurate measurement of wind speed which makes this strategy the most expensive. Generally, most of the time wind speed sensor is installed on the top of turbine nacelle and therefore it provides inaccurate wind speed data due to the constant rotation of turbine blades ahead of it [1]. At the same time another problem arises which is consistent wind speed fluctuation across the blades cannot be taken into consideration with a single measurement point even though TSR method provides the fast-dynamic characteristics along with high efficiency and faster response than other MPPT methods. Typically, TSR control is utilized for the huge wind energy conversion systems.

2.3.2 **Optimal torque control (OTC)**

As it is mentioned earlier for every wind speed, there is a specific rotor speed which is responsible for maximal value of output power. The corresponding power curve can be stored up in a lookup table or calculated to be sent in the controller memory. For every optimal power corresponding to the related rotor speed can be retrieved from the look up table. This shows clearly the current and torque reference value and because of field orientation current and torque are proportional. According to the equation (2.6) of motion we see that the difference between the turbine torque and generator torque are responsible for slow down or speed up the turbine towards MPP. Comparatively this method is slower than the TSR method since the difference between the torques is very limited. The main goal of this strategy is to control the generator torque to its optimum value for every corresponding wind speed [20]. In the following Figure 2.16 the basic concept of OTC is represented.

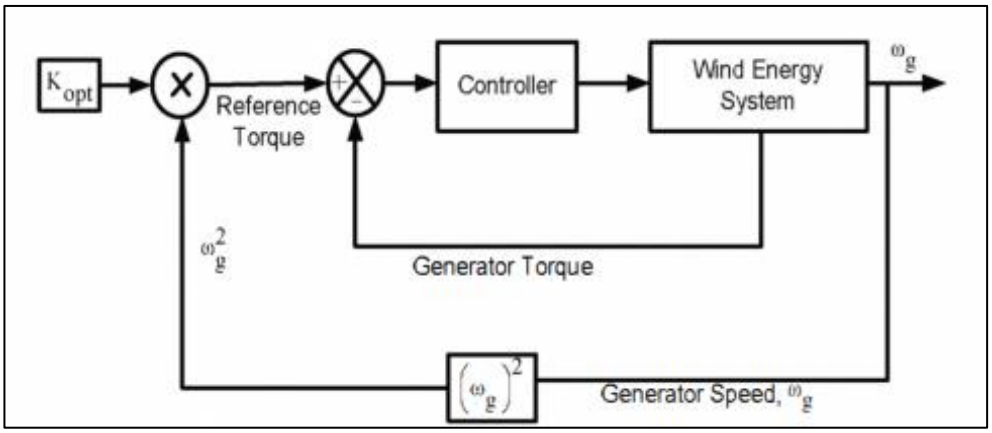

Figure 2.16 A schematic block diagram of the optimal torque control [8].

In the figure ω_g is the rotor speed and K_{opt} is a constant term which is given in the following equation.

$$K_{opt} = \frac{0.5\rho C_{p,max} r^5}{\lambda_{opt}^3} \tag{2.39}$$

The mechanical speed sensor can be avoided if we use the sensor less control scheme. One challenging task of this method is to know the optimal power curve. Therefore, the experimental values of the turbine characteristics are essential for this method. There is a common problem for both OTC and TSR control method which is the shifting of power coefficient curve with respect to the turbine blade features. Furthermore, varying condition of the temperature, air humidity, generator performance and ageing effects are some reasons for the variation in the look up table. As a result, the variations can be noticed as well in power extraction from the real MPP. The efficiency of this method is comparatively lower than the TSR control method as the wind speed is not calculated in direct way [21].

2.3.3 **Hill climb search control (HCS)**

HCS is a simple sensor less control method that can be utilized frequently in wind energy conversion systems under varying wind speeds and it is basically independent from the generator parameters, wind turbine, anemometer and wind characteristics [21]. The hill climb search control detects the deviation of generator rotor speed and output power and responds to them by adding a slight decrement or increment with the previous rotor speed reference. More clearly, the algorithm senses the output power of the PMSG through the current and voltage value which are acquired after the rectification procedure [22]. It is generally a trial and error-based control method where the reference speed is updated continuously. We can suppose that in the previous state the DC-link power is $P(k-1)$ to generate a speed difference $\Delta\omega$ and compare the recent wind power $P(k)$ with $P(k-$

1). Therefore, if the power is increased then Δω will also be increased and will be added with the previous rotor speed reference to drive the operating point towards the real MPP [17]. On the other hand, if the power is decreased then the speed reference will be decreased as well. The Figure 2.17 shows that how rotor speed is varied in HCS method to achieve the optimal power point $P_{opt}(P_{max})$.

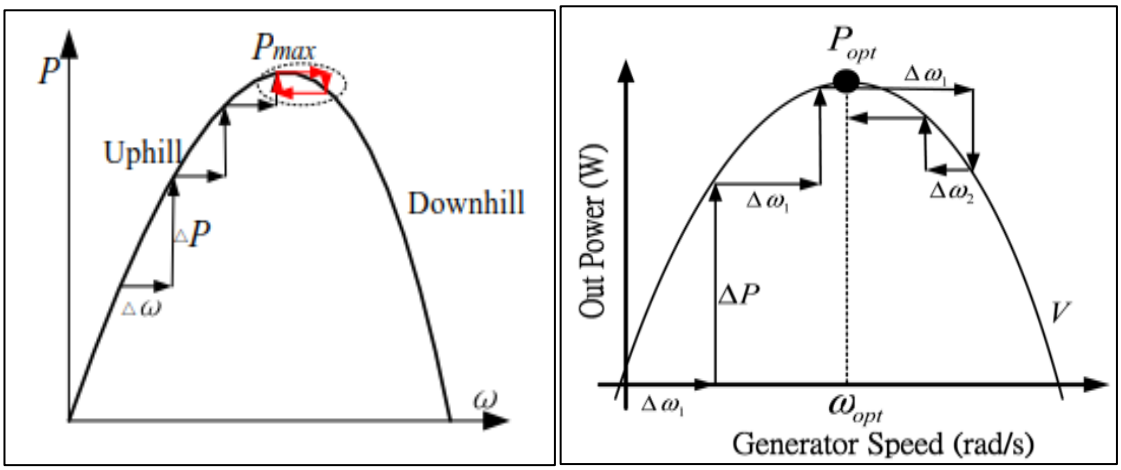

Figure 2.17 The output power of generator as a function of speed [21] [23].

In the figure ΔP depicts the power difference corresponding to its speed variation $\Delta\omega$. The drawback of this method is that it is not capable to detect the precise location of MPP. It keeps searching the MPP by continuously updating reference rotor speed. Consequently, there will be a speed oscillation around the real MPP known as *hysteresis*. However, it is possible to track the MPP precisely with using these two following rules

$$|P(k) - P(k-1)| < \delta \tag{2.40}$$

$$\left|\frac{P(k)-P(k-1)}{\omega(k)-\omega(k-1)}\right| < \theta \tag{2.41}$$

From the equation (2.41) we see that the power variation should not exceed a certain limit called δ and the equation (2.42) depicts that the slope of the power curve (gradient) must be less than a particular limit (threshold) known as θ [23].

The speed which is executed to track the MPP can be set by the step size of the generator rotor speed. A higher step size will drive the turbine faster to the maximum operating point but in result a strong hysteresis will be introduced around the MPP. Thus, it diminishes the efficiency of the MPPT. On the other hand, smaller step size increases the efficiency but minimizes the convergence speed towards the actual MPP which is not suitable for the fast-varying wind speed. To avoid this problem, a variable step size method is

needed where the step size is scaled for the variable rotor speed according to the slope of the $C_P(\lambda)$ curve [6]. It will be discussed briefly in the next sub section.

2.3.4 **Modified hill climb search control**

The conventional HCS algorithm is one of the simplest sensor less MPPT methods that is presented in the thesis. The basic concept is that perturbing shaft speed in a small step and then estimating the resulting variation of the turbine mechanical power whether it is increased or decreased. After that we can decide the next step direction of the rotor speed according to the observed power. However, for the conventional fixed step sized HCS method two types of problems arise. The large perturbation step is responsible for introducing hysteresis phenomena though the convergence speed is increased. On the contrary, the MPPT efficiency can be increased with the small step size but it slows down the convergence speed. Hence to solve this problem a variable perturbation step size is proposed by which we can improve the tracking capability of the HCS algorithm and deny the tradeoff between convergence speed and the MPPT performance. In this method the perturbation step size is determined by the slope of the turbine power ($\frac{dP}{d\omega}$) corresponding to the perturbation variable. In the beginning the step size should be larger when the MPP is far away from the operating point because of the bigger slope of the C_p curve and small slope is expected when the operating point is getting closer to the MPP since the slope of power curve is almost flattened. The maximum power point ($\frac{dP}{d\omega} = 0$) is reached when the power variation $dP = 0$ since the amount of rotor speed adjustment is proportional to the change in mechanical power [7]. The input of the hill climber is electric power that can be easily estimated from the machine side converter but also in fact the turbine power should be used for the control algorithm. Since these two powers are equal on the steady state, we must wait till the generator transient power is disappeared. Thus, only that time we can use the estimated power to calculate the next rotor speed step size for the MPPT control. It is inevitable that the wind turbine will end up to its maximum power point since no turbine data is necessary [1]. Note that, in this type of control technique two type of problems are occurred. Whenever the algorithm is switching the operating point from one C_p curve (power curve) to another under changing wind speed, the expected perturbation step size depends on the operating point region in the C_p curve. This is the reason for creating unnecessary larger or smaller step size. In addition, the Figure 2.18 shows that the power mismatches between consecutive MPPs are not same i.e. $\frac{d\omega}{dP}$ is not uniform. So therefore to eliminate the overshooting, the operating point during high wind speed we have to consider the scaling factor to the lowest $\frac{d\omega}{dP}$.

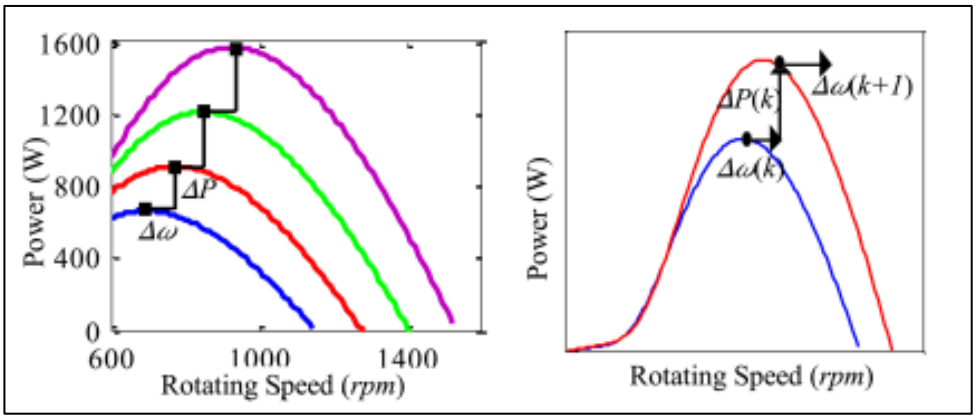

Figure 2.18 (a) power corresponding to rotor speed (b) HCS method direction misled during wind speed variation [6].

Another usual problem for this method is that HCS is blind to the wind speed variation. So, the following perturbation or step size could be misled for this fact (see Figure 2.18 (b)) [6].

3. IMPLEMENTATION METHODS AND RESULTS

The previous chapter dealt with the basic concept of the MPPT algorithms and working principle. The obtained simulated results and their further analysis along with brief description of all MPPT algorithms will be explained in this chapter. The more measurements are needed for a control scheme, the more measurement devices will be needed which will increase the total expenses and the system complexity. Furthermore, practically the precise measurements of the wind speed are challenging hence the proper filtering strategy should be utilized. To eliminate this problem different types of methods are used to measure the wind speed depending on the measurements which is easier to obtain. For example, the wind speed is calculated from the electric power of the generator considering the system losses and machine dynamics or from the optimal power curve relationship which is utilized in the optimal torque control in this thesis. Thus, the estimated wind speed can be used for the MPPT control.

3.1 Tip speed ratio control

In the point of view of implementation the tip speed ratio control is one of the easiest techniques. The measured wind speed is required as the input of the MPPT controller and the rotor speed reference is estimated from the given turbine radius and TSR with the following equation that was mentioned already in equation (2.38).

In this thesis the $C_p(\lambda)$ curve gives the optimal tip speed ratio at around 6.91. From the generator parameter datasheet, the value of nominal current can be obtained. The quadrature axis current (I_q) should be limited i.e. the output of the PI speed controller. Generally, the I_q component is in positive terms so that it is responsible for the generating torque on the opposite direction of turbine produced torque. In the case of lower TSR than the optimal TSR, the generator torque is set as zero resulting in speed up the turbine. Thus, the set point would be gained with the help of increasing turbine torque. But just before the maximum power point is achieved, the generator torque will be developed again till both are in same value at the optimal tip speed ratio.

The current reference in the rectifier can likewise end up noticeably positive by which machine torque is created in PMSG which acts in opposite direction from the turbine torque. Thus, along these way, the PMSG can assist the turbine torque with speeding up the rotor. It is possible to achieve MPP quickly and grid side electric power is used to improve the acceleration of the control.

In the Simulink model the measured wind speed is used as the input of the wind turbine that drives the PMSG. In TSR method this value can be used directly as well. Even though it is not typical for the wind speed sensor, it could be only a justification to investigate the performance of the speed control. To make it more realistic it is logical to add an error signal as well with the real wind speed data.

3.1.1 Simulation model

The previous chapter describes the vector control of the PMSG elaborately. The simulation time for the current control loop (inner loop) is smaller (in milliseconds) since it is a faster procedure. On the other side, the speed control is a much slower process (in seconds) therefore it is considered that the torque control should be infinitely fast process. Therefore, the simulation time for this should be decreased. Consequently, because of the field orientation the generator torque is proportional to the quadrature axis current I_q at any time.

The Figure 3.1 shows the simulation model of the TSR control scheme. The model was tested for both constant and variable wind speed values. The variable wind speed data was taken from the solar laboratory of the Tampere University of Technology, Finland. The sampling frequency of the rapidly varying wind profile is 0.02 Hz which means in every fifty second the wind speed changes. However, this fluctuation takes place in very limited ranges. This wind profile will be applied for checking the performance of the Simulink model of all MPPT control strategies. The lower block is the wind turbine model in which the wind speed value and actual rotor speed are given as inputs. The PI controller generates the reference value of the q-axis stator current. The parameters of the speed controller are tuned according to the *Ziegler-Nichols* rules which is trial-error method for PID controller. The reference rotor speed and measured rotor speed are compared and the error result is fed to the speed controller. As it was mentioned earlier the first one was calculated from the TSR and given wind value. The current reference is then transformed into the generator torque T_g by multiplying a generator torque constant denoted as K_t. In the following equation (3.2) the reluctance magnetic term is neglected.

$$T_g = \frac{3}{2} N_p \psi_{PM} I_q = K_t I_q \tag{3.1}$$

In which

$$K_t = \frac{3}{2} * 6 * 3.1851 = 28.6659 \text{ (Wb)} \tag{3.2}$$

The whole mechanical equation is applied as the integrator of the torque variance to estimate the rotor mechanical speed where the total inertia J was considered. After that, the rotor speed is fed back to the PI controller and to the wind turbine model. Notice that,

here the system mechanical friction was not considered due to the direct drive feature of PMSG.

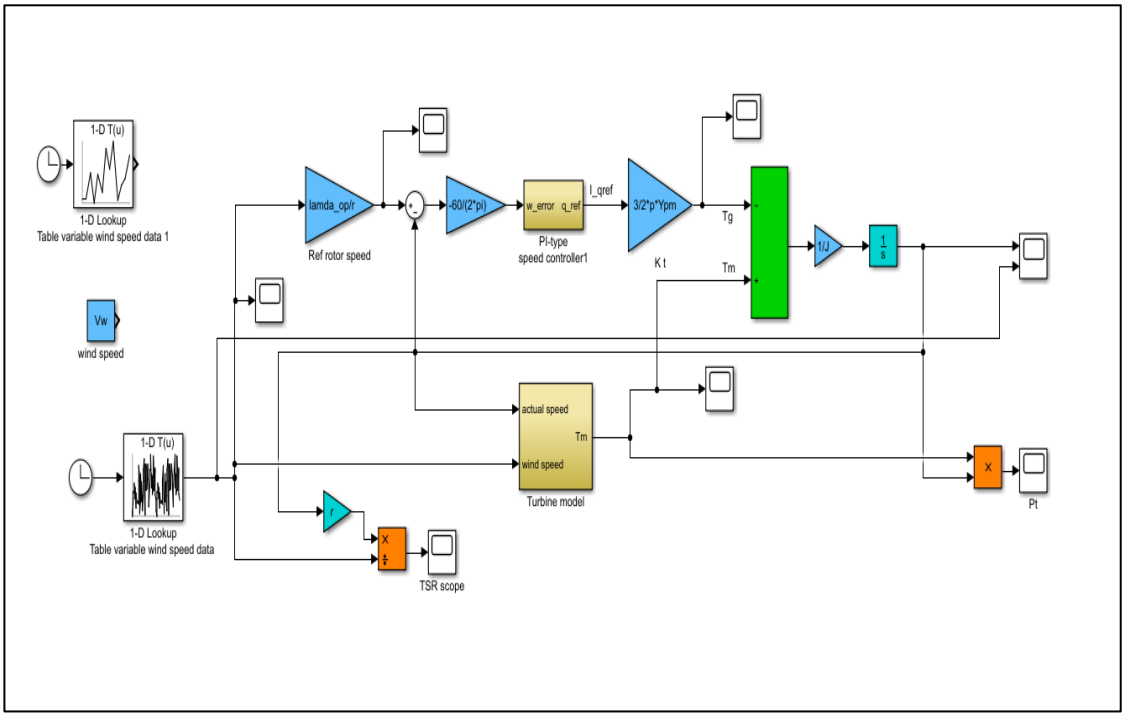

Figure 3.1 TSR control loop Simulink diagram.

3.1.2 **Simulation results**

In the following figures the simulation results of the TSR control system is presented with the stable wind speed (v_w) value 10 m/s. We see from Figure 3.4 in the beginning of the simulation, the rotor speed fluctuates which is due to the difference of the generator and turbine torque. The turbine has to be accelerated slowly to reach its actual MPP and the controller set the generator torque value at zero. Whenever the turbine nearly achieves its MPP, the generator torque starts to increase until it becomes equal to the turbine torque. Consequently, the optimal rotor speed value is obtained which is 14.5 m/s. The following figures show that the rotor speed and the turbine torque is in stable because of the stable wind speed. However, how fast the MPP is reached is mainly determined by the system inertia. It is possible to know whether the algorithm is working properly by checking the TSR. We know that in our case the optimal tip speed ratio is 6.91. The Figure 3.3 proves that optimal TSR is achieved and the algorithm is implemented properly to achieve optimal power operation. Furthermore, it is seen from the figures 3.5 and 3.6 that at optimal TSR both turbine and generator electrical torques are equal.

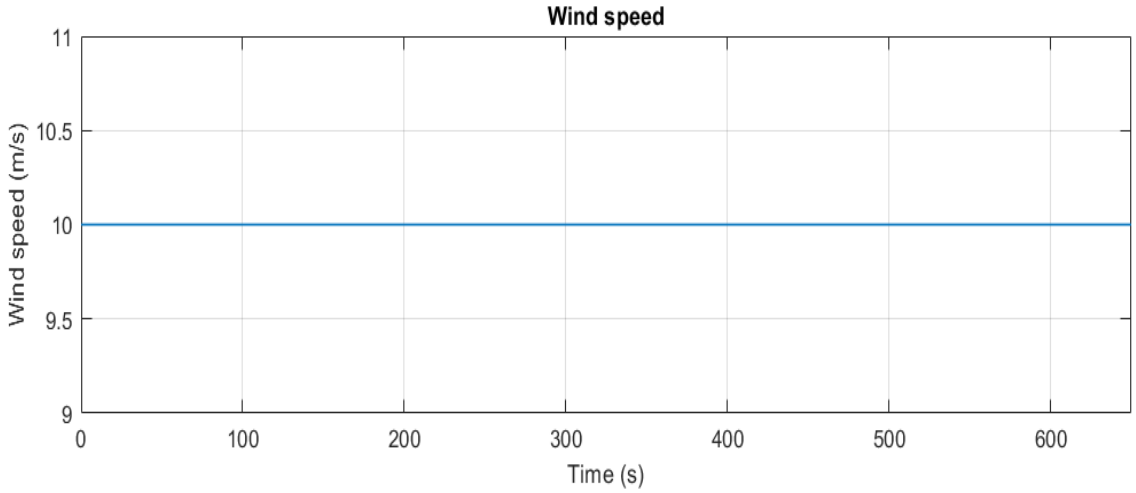

Figure 3.2 Fixed wind speed value of 10 m/s.

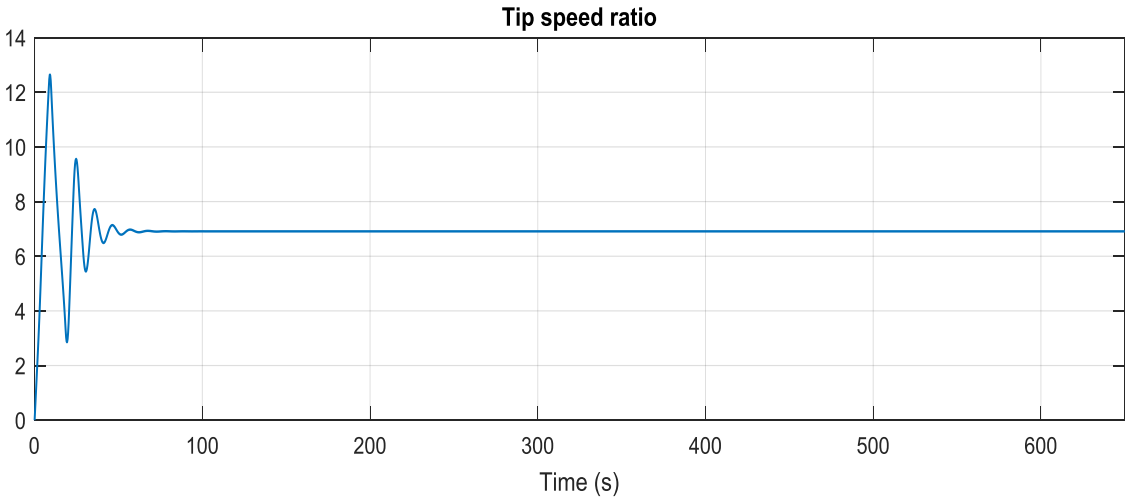

Figure 3.3 Simulated TSR value as a function of time.

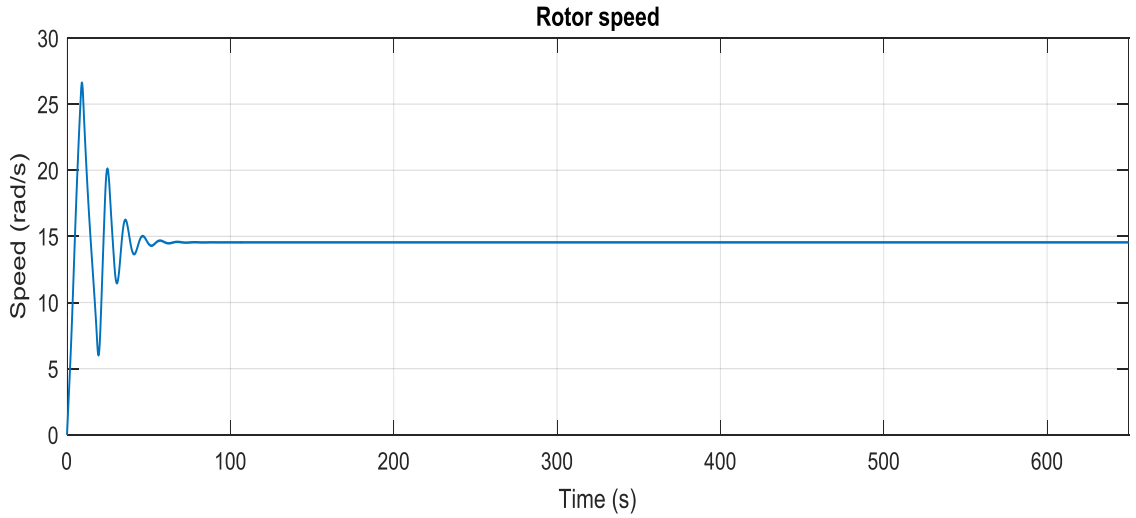

Figure 3.4 Actual rotor speed in rad/s as a function of time.

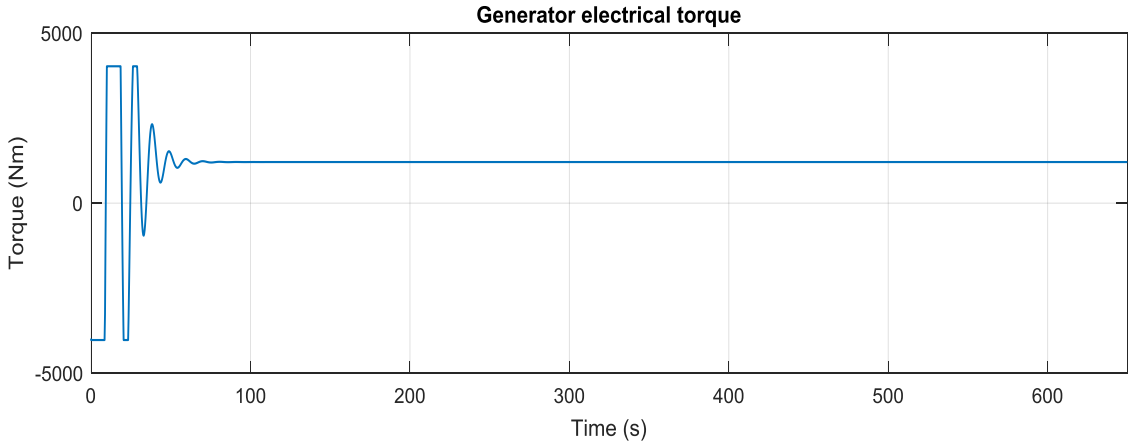

Figure 3.5 Generator torque $\boldsymbol{T_g}$ in Nm.

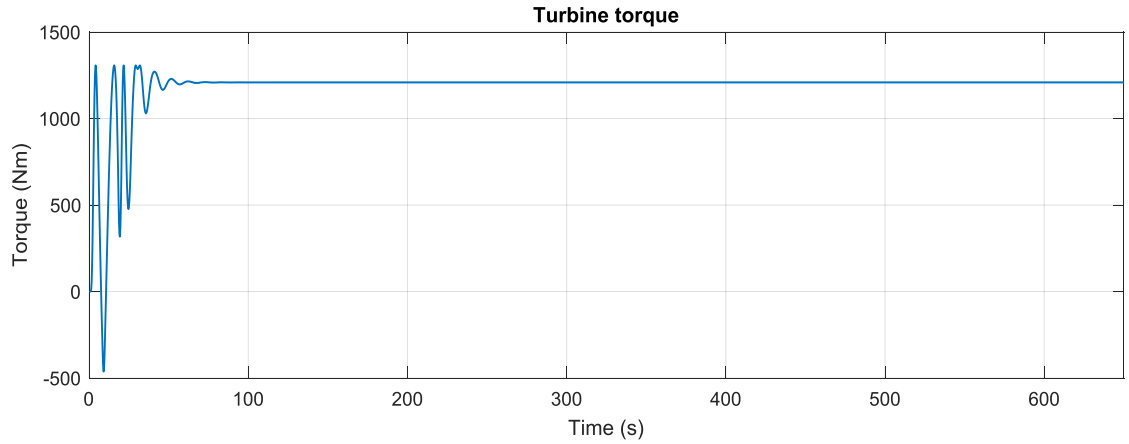

Figure 3.6 Turbine torque $\boldsymbol{T_m}$ in Nm as a function of time.

In the figures from 3.7 to 3.12 the simulation results of the variable wind speed of sampling frequency 0.02 is shown. The wind speed data was taken in every 50 seconds and they can be uploaded into the Matlab 1-D lookup table. The same characteristics arises with this variable wind speed as we have seen with the fixed wind speed i.e. the rotor speed always tries to follow the variation of the wind speed along with a small transient which is actually determined by the system inertia. Due to the high inertia of the whole system the generator torque and rotor speed respond slowly corresponding to the wind speed variation. If we closely observe the rotor speed curve from 90 second to 450 seconds, it proves that the rotor speed variation is in limited range. In the Simulink model, the current limiter utilized in the speed controller helps the generator torque to be limited in its rated value while the turbine is slowing down. The rotor speed is always within the rated speed range though the turbine experiences sudden wind speed variation.

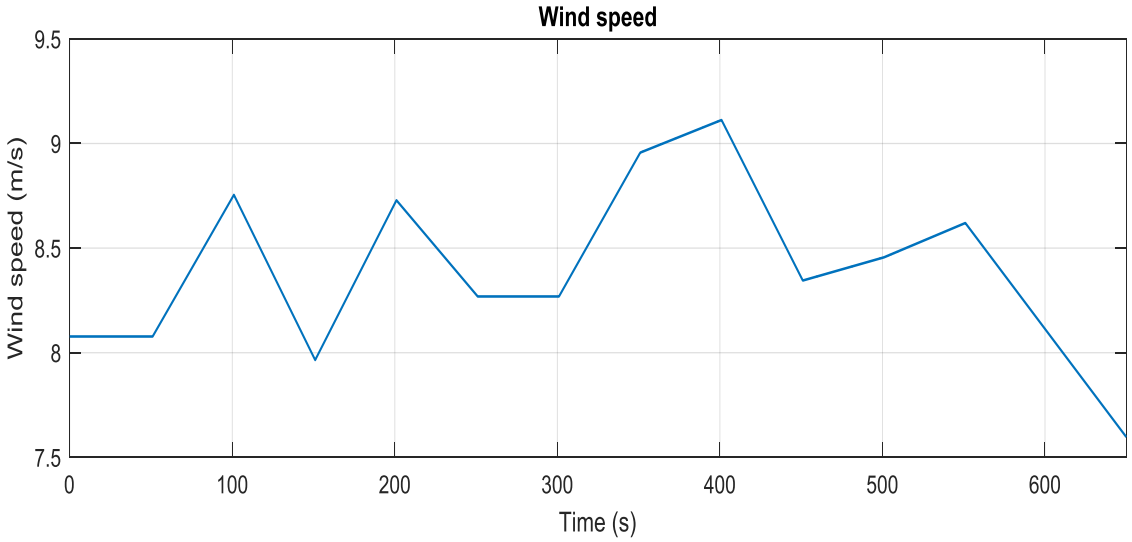

Figure 3.7 The variable wind speed data in m/s.

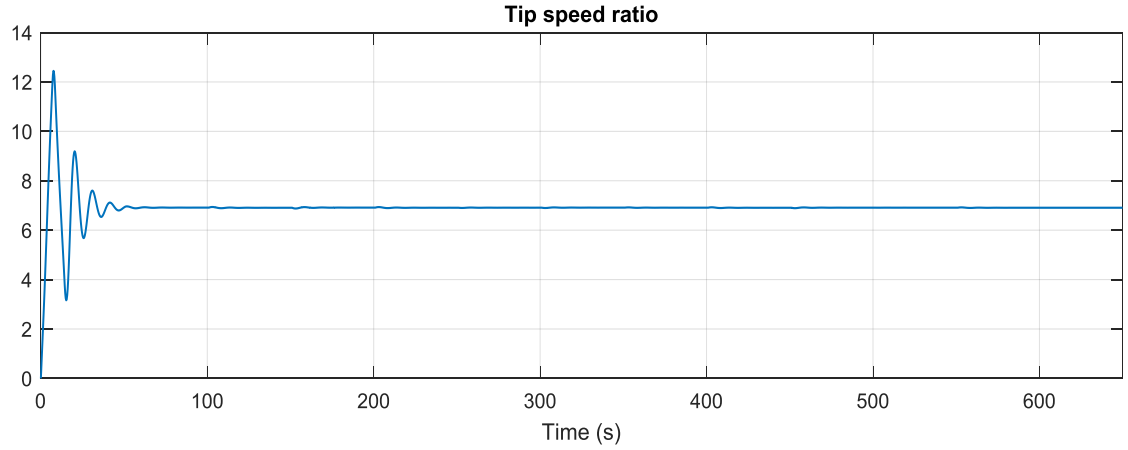

Figure 3.8 Simulated TSR value as a function of time.

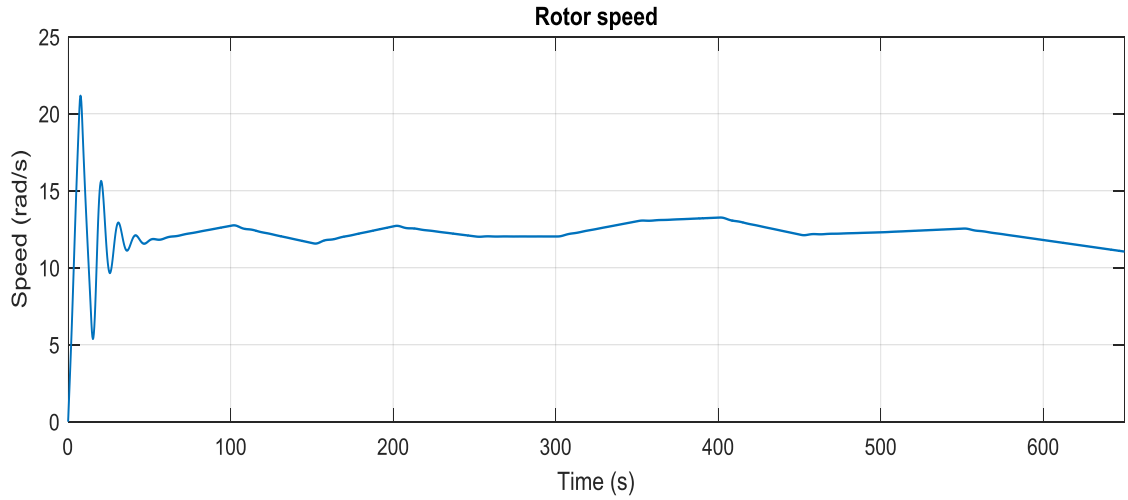

Figure 3.9 The rotor speed in rad/s as a function of time.

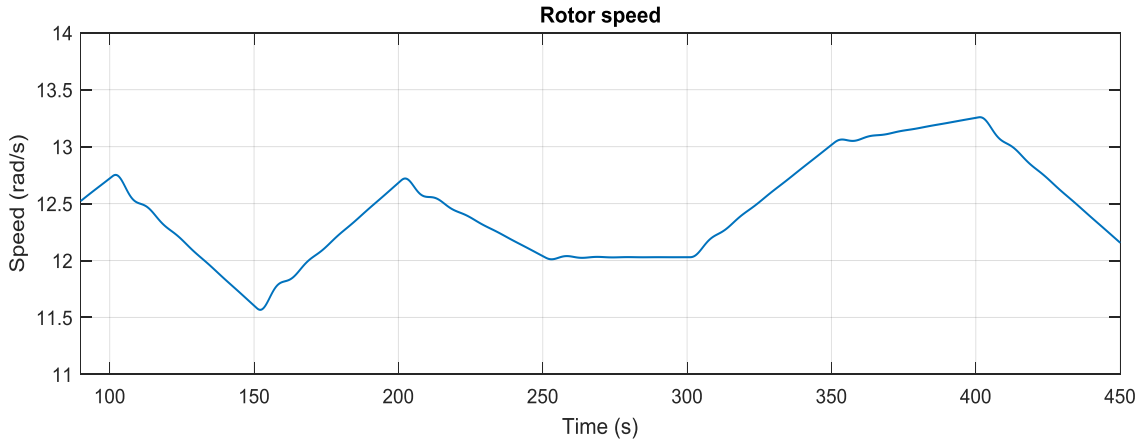

Figure 3.10 The closer view of rotor speed in rad/s from 90 to 450 second.

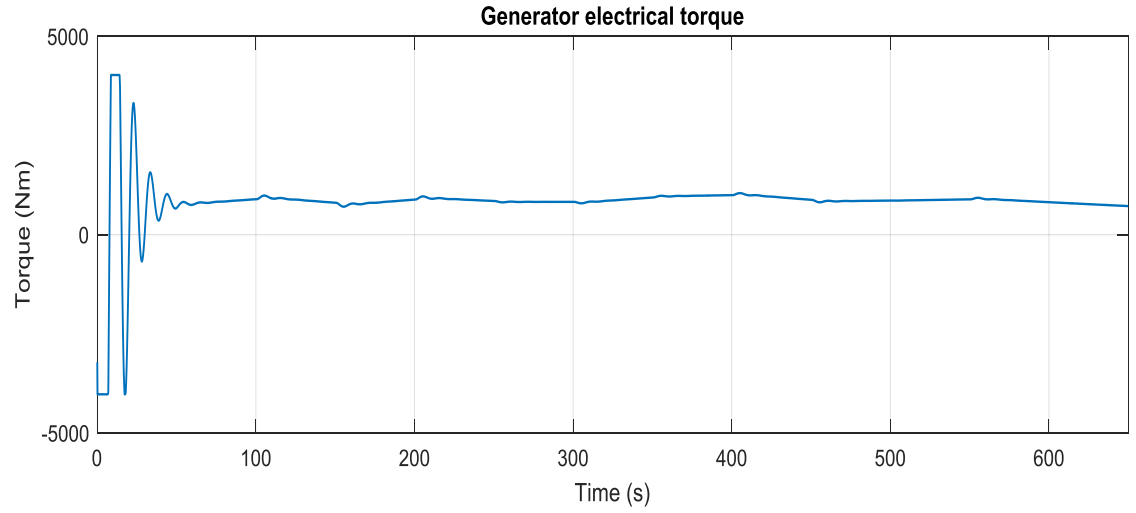

Figure 3.11 The generator electrical torque $\boldsymbol{T_g}$ in Nm with respect to time.

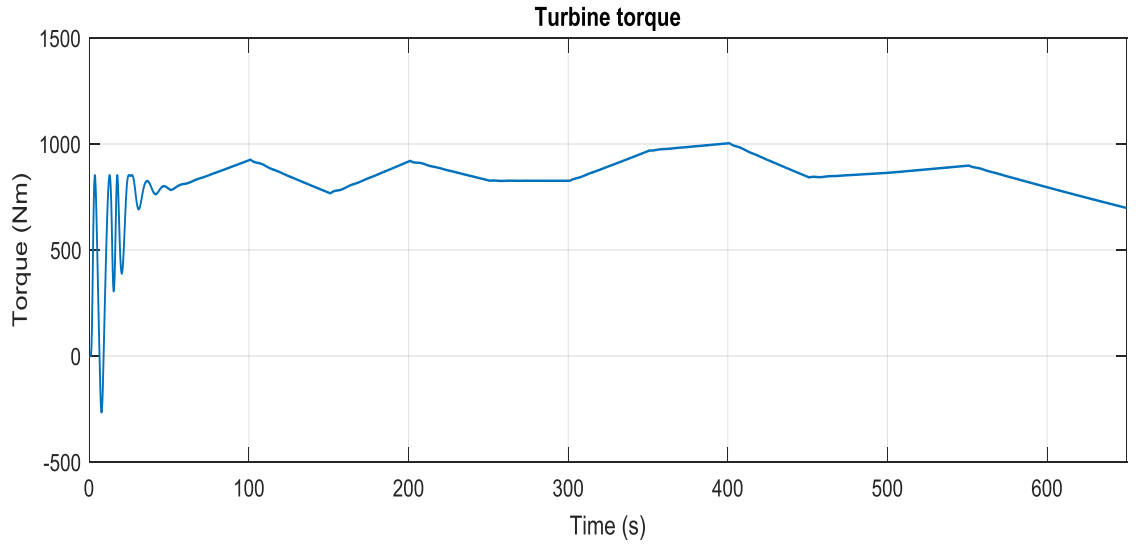

Figure 3.12 The turbine torque $\boldsymbol{T_m}$ in Nm as a function of time.

The parameters that have been used for the PI controller are Proportional value $P_i = 1$, integral value $T_w = 0.5$.

In every transient due to the wind speed variation the generator torque and the rotor speed are changing but it takes few seconds in order to follow the wind speed variation due to high inertia. Contrary we can notice that the turbine torque responds immediately with the wind speed variation. The closer view of the rotor speed shows that for a specific wind speed there is an optimum speed where the generator operation is stable and produce the optimum power. The TSR for stable and variable wind speed seem to be in its optimum range around 6.91 which means the algorithm is working accurately (see Figure 3.3 and 3.8).

3.2 Optimal torque control

As it was mentioned that optimal torque control is one of the most frequently used and simplest MPPT control strategies. The main concept behind is that in every specific rotor speed ω_T an optimum power P_{opt} exists which is known as optimal power curve relationship. In this curve every certain point relates to a specific wind speed that is unknown. With the help of knowing the $C_P(\lambda)$ curve of turbine we can calculate wind speed from this relationship. Another way could be using the experimental procedure where the MPPs can be known and fitted with polynomial function.

In the experimental setup the wind turbine emulator gives the optimal power values from the programmed $C_P(\lambda)$ curve. From the following relationship the maximum power output happens when the wind turbine is running at maximum power coefficient $C_{P,max}$.

$$P_{opt} = \frac{1}{2}\rho\pi r^2 C_{P,max}\, v_w^3 \tag{3.3}$$

Since the rotor speed and the wind speed are related to each other through TSR, the wind speed v_w can be calculated turbine running at the MPP as shown in the following equation

$$v_w = \frac{r\omega_T}{\lambda_{opt}}. \tag{3.4}$$

Thus, the equation (3.4) can be substituted to the (3.3) for executing the maximum power points

$$P_{opt} = \frac{1}{2}\rho\pi r^2 C_{P,max} \left(\frac{r}{\lambda_{opt}}\right)^3 \omega_T^3 = K_{opt}\omega_T^3 \tag{3.5}$$

where $K_{opt} = 5.6983$ is from the machine technical specification datasheet.

Thus, the optimal torque can be computed in the same manner as

$$T_{opt} = K_{opt}\,\omega_T^2. \tag{3.6}$$

The torque is dependent on the quadrature axis stator current I_q. Due to the field orientation the relationship is

$$T_{opt} = I_{q,opt}\,K_t. \tag{3.7}$$

The relationship between equation (3.6) and (3.7) gives directly the current reference value for the PI speed controller. In more precisely the measured rotor speed gives I_q value.

$$I_{q,opt} = \frac{K_{opt}\,\omega_T^2}{K_t} \tag{3.8}$$

The wind turbine torque is always a function of the rotor speed and wind speed while generator torque can be obtained from the optimal torque curve. The figures 2.3 and 2.4 in chapter 2 present how the MPP is occurred. Since the machine has high inertia the rotor speed cannot be increased or decreased while wind speed varies suddenly. Therefore, the generator torque remains stable for a while but the turbine torque varies instantly according to the wind speed. This difference between the torques will accelerate or deaccelerate the wind turbine. Assume that when the wind speed is decreasing the turbine speed and the generator torque are also decreasing. As a consequence, the turbine torque is also getting lower. Eventually the MPP is occurred when both torques will be equal.

3.2.1 **Simulation model**

In the Figure 3.13 the Simulink model of the optimal torque control is shown. The turbine model block is responsible for calculating the turbine torque from the beginning of the wind speed and the rotor speed. The generator torque is estimated from the equation (3.7). After that the inertia J will accelerate or deaccelerate with respect to the difference of the both torques. The Simulink model is tested for both stable and variable wind speed profile.

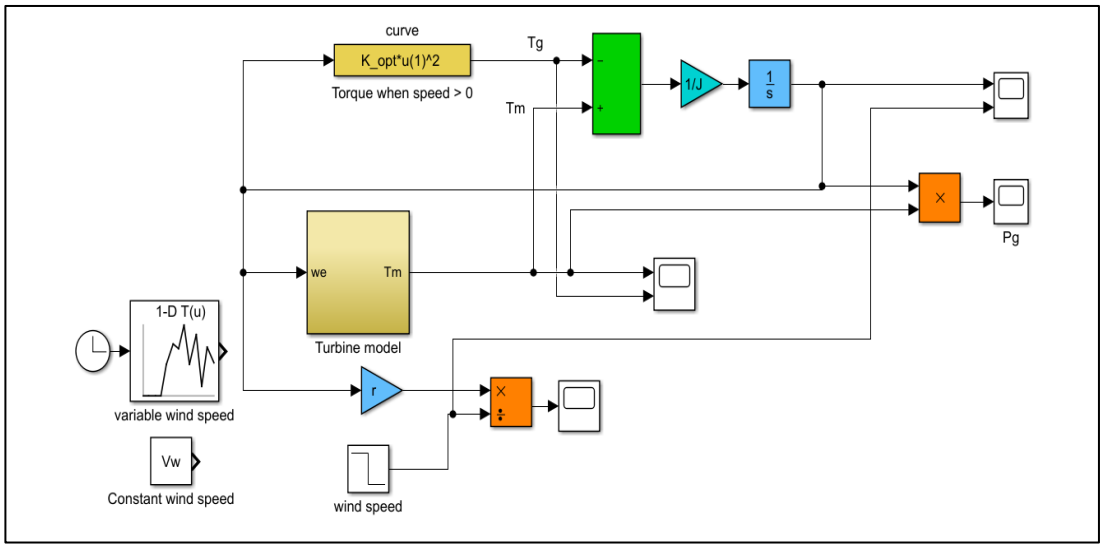

Figure 3.13 Simulink model of optimal torque control (OTC).

3.2.2 **Simulation results**

All the simulated results are presented in the following figures for OTC. At first the Simulink model is tested for the stable wind speed of 10 m/s in the initial 400 seconds. We see that the turbine starts to accelerate in order to reach in its optimal TSR (see Figure 3.16). We have made a step where the wind speed suddenly drops at 8 m/s. In the same manner the TSR again achieve its optimum value after experiencing a transient for few seconds. Note that, comparison based on the simulated results for the OTC, the settling time is longer than the TSR control. The Figure 3.16 proves that a step of 2 m/s leads to delaying the settling time approximately 30 seconds. This is actually very slow process for such small wind turbine. However, this slow reaction could be explained this way: when the turbine experiences a step of wind speed, the wind turbine torque increases instantly but the generator torque changes very slowly (see Figures 3.17 & 3.18). This is because of the generator rotor speed cannot change immediately due to the high inertia of the machine. As a result, the difference between these two torques are comparatively small. Therefore, the acceleration of the turbine remains in very limited range. On the other hand, in the TSR control the generator torque T_g are set to zero and thus the differences between the torques are getting smaller. It means that the generator speed is approaching to its MPP. For this simulation model, first the generator should be started as a motor. How fast the rotor speed reach to its MPP, it depends on the initial speed of the rotor. More clearly for the higher value of the initial rotor speed, the settling time for stability becomes smaller. It is noticeable from the results is that the generator torque T_g is a quadratic polynomial function of the generator speed. Furthermore, we observe that the turbine torque changes in the similar way of corresponding rotor speed. But whenever a transient is occurred the torque differences of the system is slowly getting smaller till both

of them are equal. Eventually at that time turbine achieve the MPP and the system starts to operate in stable region.

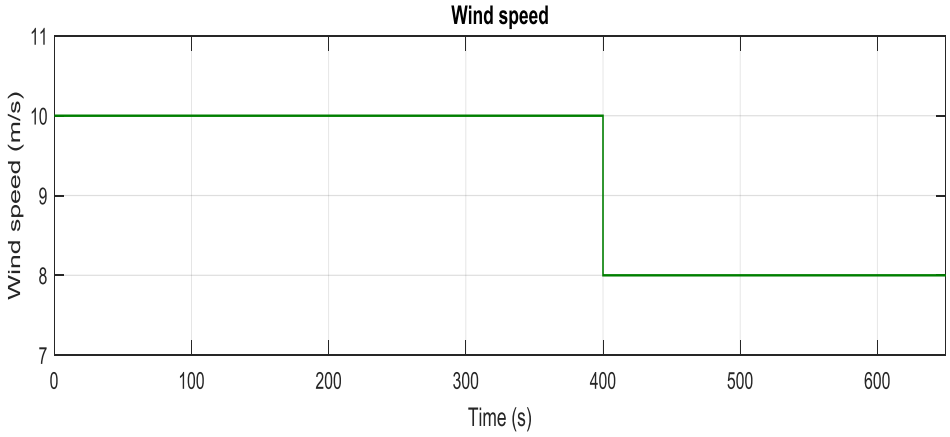

Figure 3.14 Wind speed in m/s.

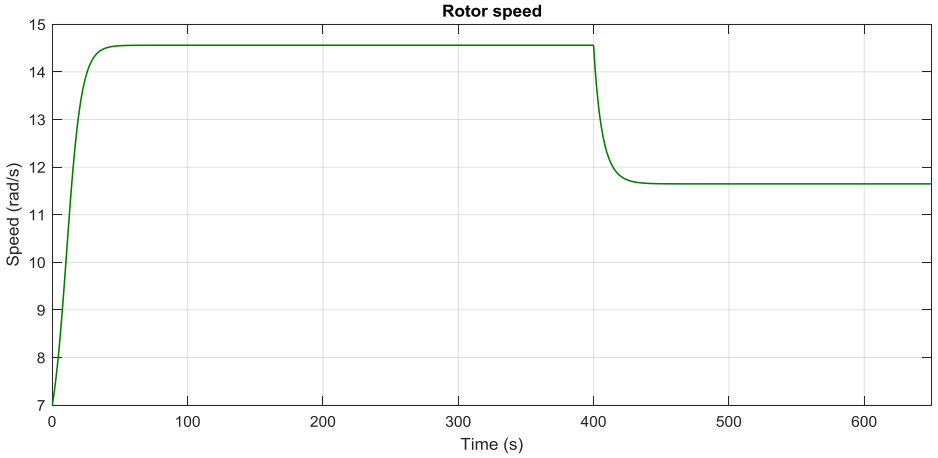

Figure 3.15 Actual rotor speed in rad/s with respect to time.

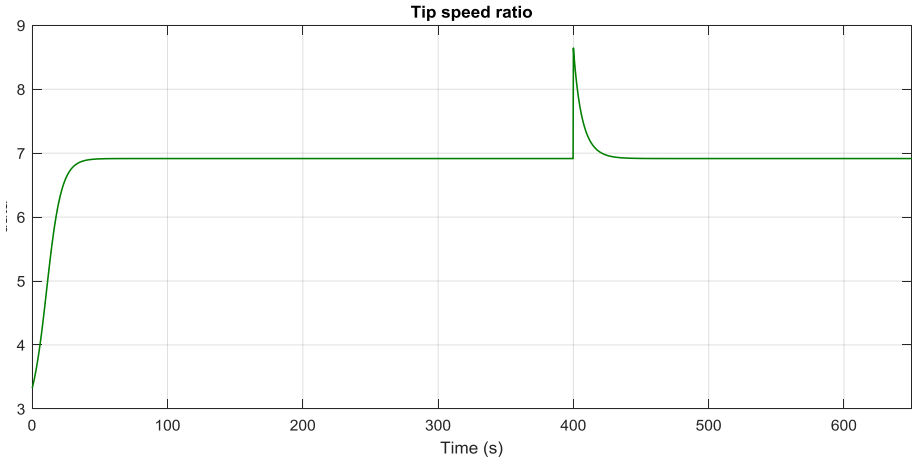

Figure 3.16 Simulated value of Tip speed ratio (TSR) of OTC control.

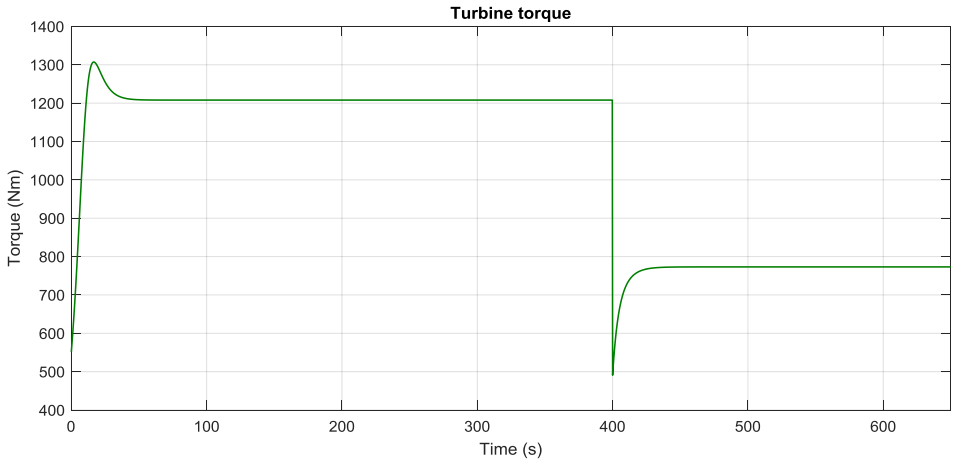

Figure 3.17 The turbine torque $\boldsymbol{T_m}$ in Nm with respect to time.

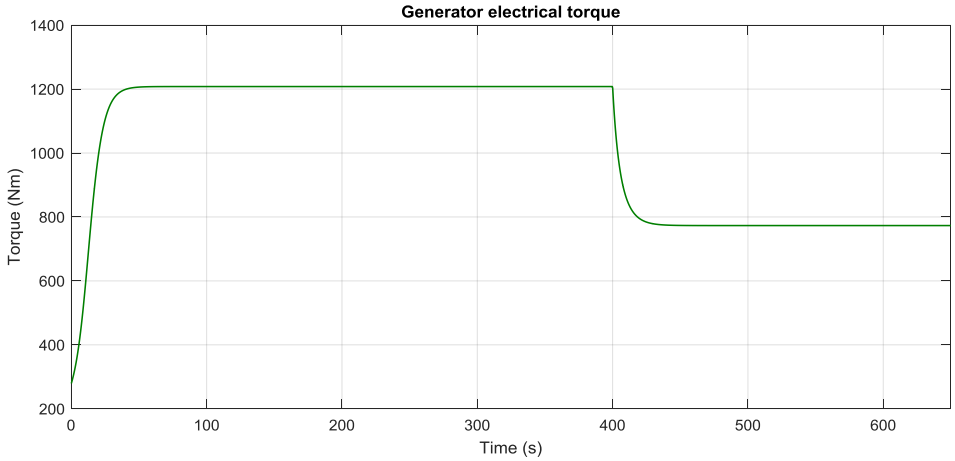

Figure 3.18 The generator torque $\boldsymbol{T_g}$ in Nm as a function of time.

Now the Simulink model is tested with the variable wind speeds and the related results are shown from Figure 3.19 to 3.24. The wind speed variation was taken in every 50 second. We see that for the initial 150 seconds the wind speed is kept stable. The rotor speed starts to increase slowly likewise the generator torque from its initial set value 7 m/s and stabilized to its optimum speed value including gaining the optimal TSR. As we know the TSR is inversely proportional to the wind speed. When the wind speed changes slowly from 150 seconds to 250 seconds, the TSR varies slowly and always around the optimal range. On the contrary, we see the different characteristics for sudden wind speed variation such as from 300 seconds to 400 seconds. Basically, we can assume the sudden wind speed changes as a step change which is described already. The rotor speed follows the wind speed variation but rotor speed as well as generator torque change slowly due to inertia (Figure 3.22 & 3.23).

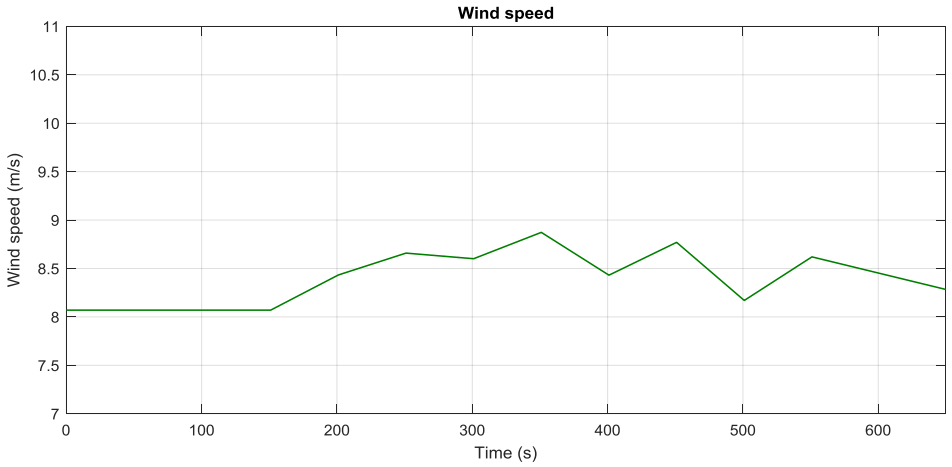

Figure 3.19 Variable wind speed data in every 50 seconds in m/s.

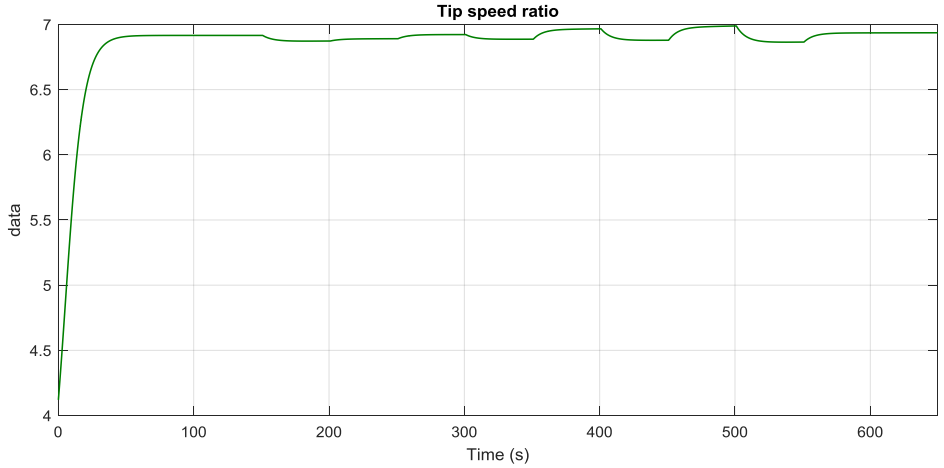

Figure 3.20 The simulated TSR value.

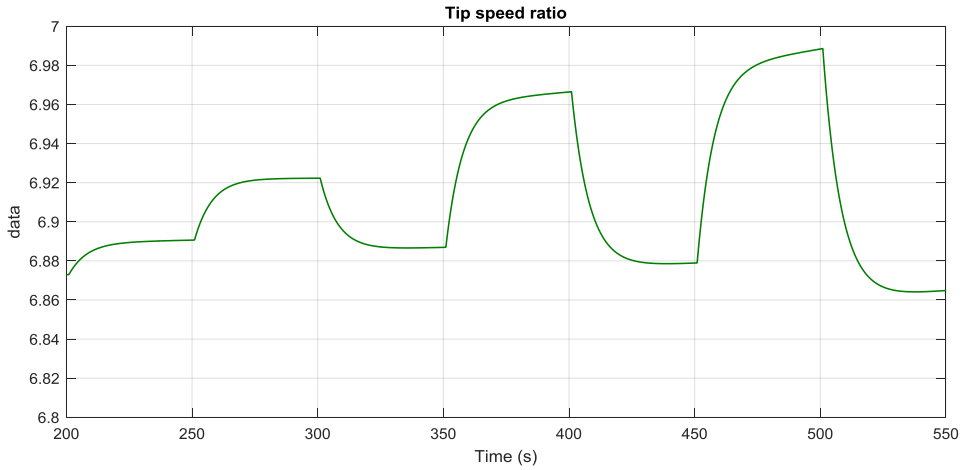

Figure 3.21 The closer view of the TSR from 200 second to 550 second.

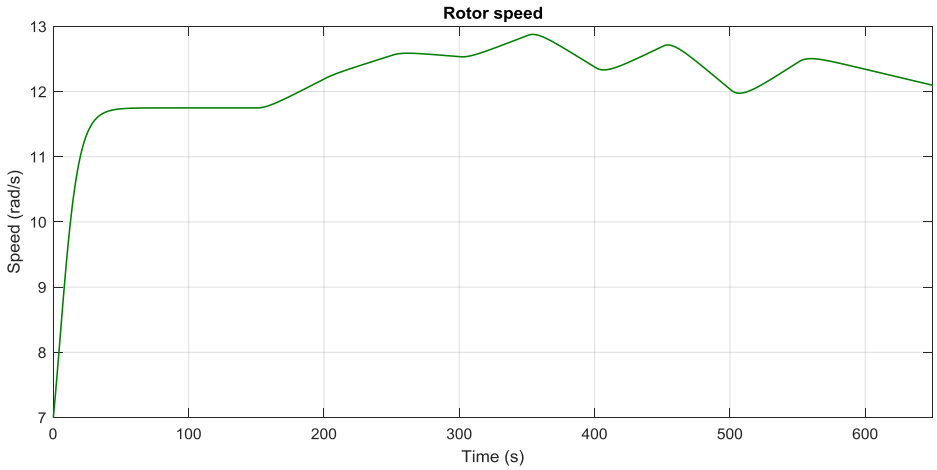

Figure 3.22 The corresponding rotor speed in rad/s.

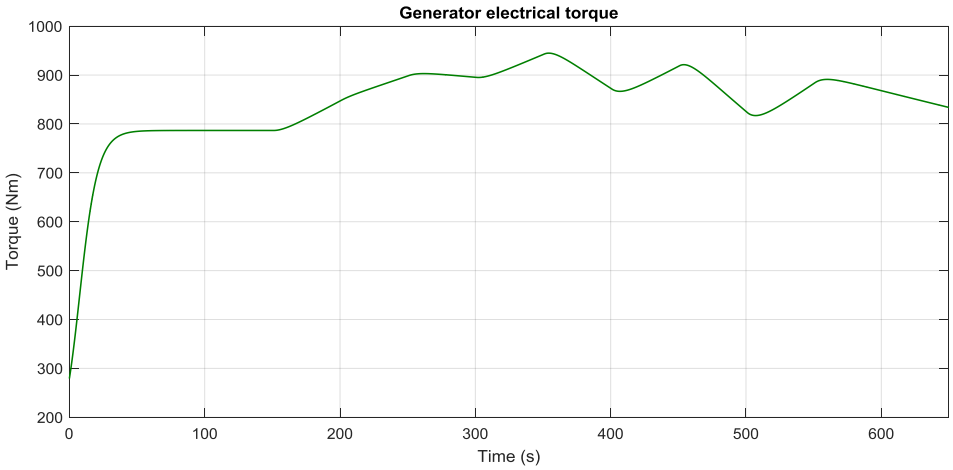

Figure 3.23 The generator torque $\boldsymbol{T_g}$ in Nm as a function of time.

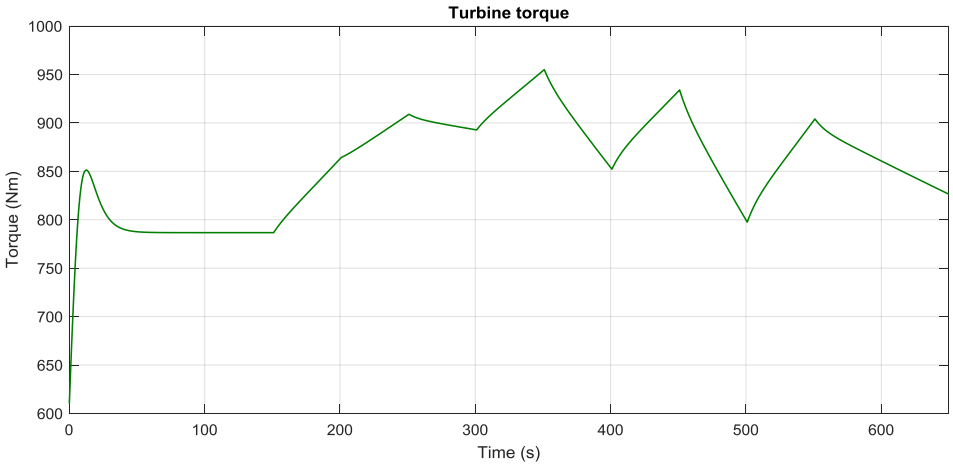

Figure 3.24 The turbine torque $\boldsymbol{T_m}$ in Nm.

3.3 Hill climb search control

The hill climb search control algorithm is a MPPT technique where the turbine data is not required to detect the location of the MPP. Additionally, it can enable the compensation for the variation of turbine features and other exterior dissimilarities like air pressure and temperature variation. The main concept behind this scheme is that the HCS controller detects the rotor speed and power variation. Based on the increment or decrement of those differences the controller decides on which portion of the C_p curve the turbine is working by that time. Thus, how we can determine instantaneously on which side the operating point is located from the MPP. According to this information we can update the reference value $\omega_{ref}(k)$ for the speed controller with small fixed step ω_{step}. The whole idea is presented with the flow chart in Figure 3.25 for the better understanding.

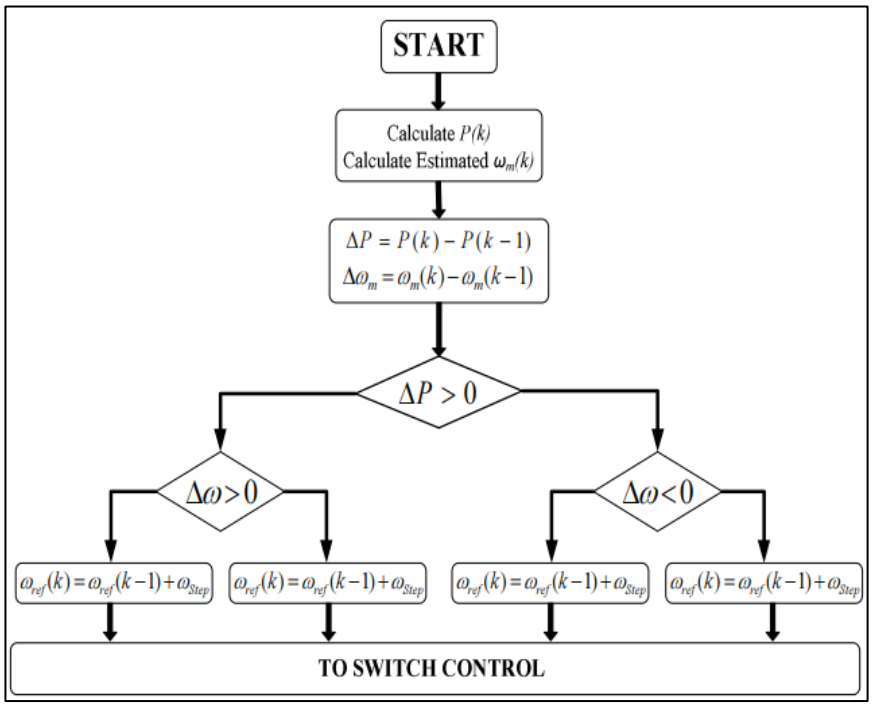

Figure 3.25 Flow chart for the HCS method [5].

For example, if both the power and rotor speed are increasing the HCS controller will sense that the turbine is moving forward to the MPP. Hence it will increase the speed reference value with small steps to speed up the turbine and thus a new cycle will be started. We can decide how large the step size should be for the proper tracking of the MPP. Because the larger step will help the controller to react fast but at the same time it will introduce the oscillation around the MPP. We know that the actual control mechanism is implemented in MPPT controller which controls the speed of the turbine. The following conditions are implemented inside the MPPT controller.

$$\omega_{step} = sign\,(\Delta\omega_m).sign\,(\Delta P) \tag{3.9}$$

$$\omega_{ref}(k) = \omega_{ref}(k-1) + \omega_{step} \tag{3.10}$$

In the above equations and Figure 3.25, ΔP and $\Delta\omega_m$ depict as the turbine power and rotor speed variation and $P(k)$, $P(k-1)$ are present and previous turbine powers respectively. Likewise, $\omega_m(k)$ and $\omega_m(k-1)$ are the present and previous rotor speeds respectively. Here, the PI controller parameters are slightly modified that was used in the TSR control algorithm. In the TSR control the goal was to reach at MPP as soon as possible. On the other hand, in the HCS control algorithm, the additional condition arises that the q-axis reference value must be a stable value in regime to eliminate large fluctuations in the electric power. The PI controller is tuned to reduce the fluctuation in the output signal.

As we know that $C_p(\lambda)$ curve provides the relationship between the rotor speed and turbine power for a certain wind speed. In steady state condition the generator power is almost equal to the turbine power. Only a little fraction of mismatches is considered which is determined by the generator efficiency and the system mechanical friction. However, WECS based on the PMSG has a very low friction coefficient because of the direct driven construction. Besides, the PMSG has higher energy densities. Therefore the difference between turbine and generator power very small.

In each time whenever a new reference step value is applied the generator electric power will experience a transient for few seconds. This transient remains until the rotor speed is stabilized for a new speed reference value. When the electric power is stabilized only that time we can use the measured turbine power inside the controller for calculating the new step size for the rotor speed reference. Therefore, the HCS strategy is a slow control method since the time between two calculation cycles could be few seconds [1].

There is one way to improve the efficiency of the HCS as well as eliminating the oscillation around the maximum power point. If the mismatch between two successive power outputs is lower than a certain threshold we can utilize the previous rotor speed reference as its new reference value. Thus, we can eliminate the hysteresis around the MPP to get the stable operation of the system.

3.3.1 Simulation model

In the following Figure 3.26, the Simulink block diagram of the HCS control method is presented. The whole process initiates with calculating the rotor speed and the turbine power. These two values are the input for the MPPT controller in order to estimate the new rotor speed reference. During the calculation process the previous values of the power and rotor speed should be saved in the memory block. After that the new speed reference will go through the PI speed controller that was basically used for the tip speed

ratio control. The parameters of the speed controller were slightly changed for the use of the HCS control. The following two conditions are checked in the MPPT controller.

$$P_{present} - P_{last} > 0 \tag{3.11}$$

$$\omega_{present} - \omega_{last} > 0 \tag{3.12}$$

In which $P_{present}$ and P_{last} are the recent and previous powers. Likewise, $\omega_{present}$ and ω_{last} are the present and previous rotor speed respectively. By checking the above condition, the controller will know on which side of the C_p (λ) curve the turbine is operating.

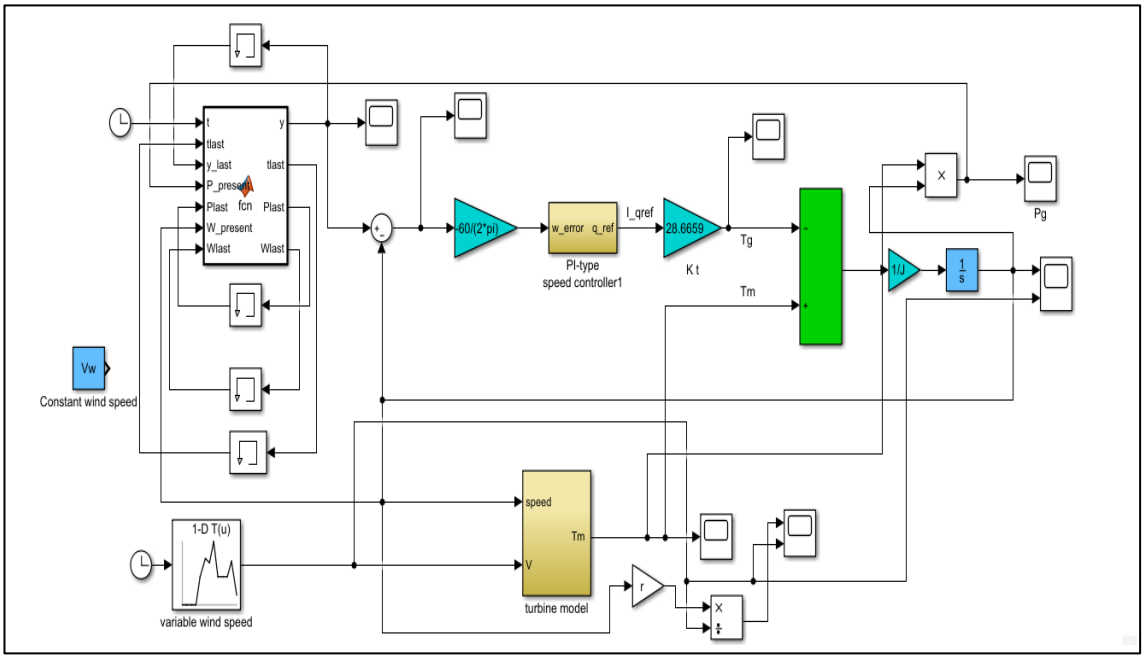

Figure 3.26 HCS control Simulink block diagram.

As we have observed in the TSR control method the MPP was achieved as fast as possible. But in the HCS control method the quadrature axis reference value should be a stable value in steady state so that large oscillations can be avoided in the electrical power.

3.3.2 **Simulation results**

The simulated results are presented in the following figures for fixed and variable wind speed. At first the model was tested with the step wind speed value where the initial wind speed is 10 m/s and after 300 seconds the wind speed drops at 8 m/s. The whole simulation was run for the 650 seconds. In the HCS method the step size of the rotor speed reference was selected 0.005. At first it is noticeable that the settling time is much longer than the TSR and OTC method. The turbine reaches to its MPP for the initial 10 m/s wind speed.

From the simulated results provided with step wind speed value we see that the MPP was not tracked preciously (see Figure 3.28 & 3.30). Since the step size was increased or decreased with a fixed small value (0.005 rad/sec) so it provided a small oscillation in rotor speed and this step size is large enough to sense the power differences properly. The convergence speed of the MPPT could be increased by increasing the perturbation step size i.e. rotor speed reference step size. As a consequence, it will introduce larger oscillation of rotor speed and decrease the efficiency of the control method. The coverage of the rotor speed for 10 m/s wind speed is in between 14 m/s and 15 m/s which is reasonable (see Figure 3.29). Likewise, for 8 m/s wind speed the rotor speed coverage is in between 11.2 m/s and 12.2 m/s. That means for the stable operation and extracting the optimum power from the specific wind speed the turbine must be run in these speed ranges. As because of the high inertia of the machine the rotor speed and generator torque cannot drop instantly to its optimum range for the 8 m/s wind speed. Therefore, there is a certain time delay (around 40 seconds) for the rotor speed to operate back into the stable region. After this transient it is clearly observed the generator torque, turbine power and the rotor speed stabilized into the steady state (regime). In addition, we can see that the TSR is oscillating around its optimum value that is 6.91. It means the system is extracting the maximum power with that wind speed. If the speed of the turbine has to be increased, then the generator torque should be set in zero value in order to make the electric power zero. On the other hand, if the turbine speed need to be decreased the generator torque should be restricted in its rated range. It is important to decrease the sampling period, but it will create longer settling time and the overshooting during the variable wind speed. This is because the generator power cannot arrive in its regime within sampling time. There is another adverse effect of the smaller sampling time i.e. faster oscillations rotor speed around MPP. This is resulting in the decreasing of the efficiency of MPPT.

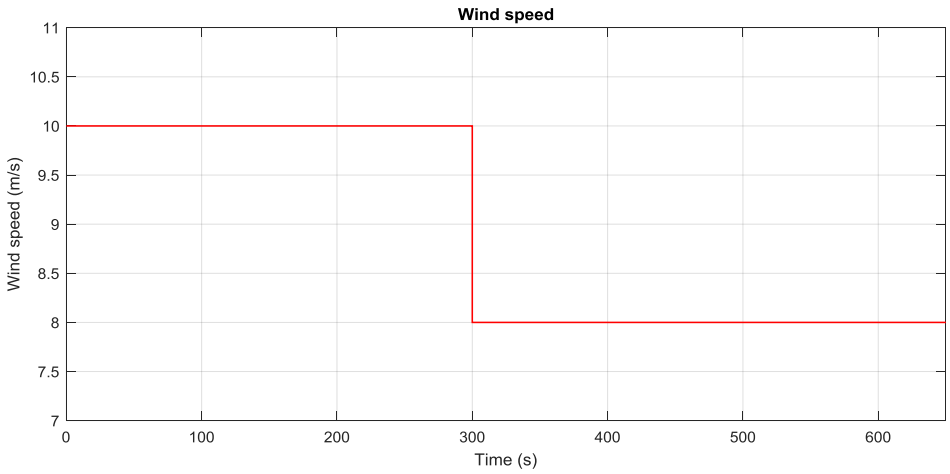

Figure 3.27 The provided wind speed value in m/s.

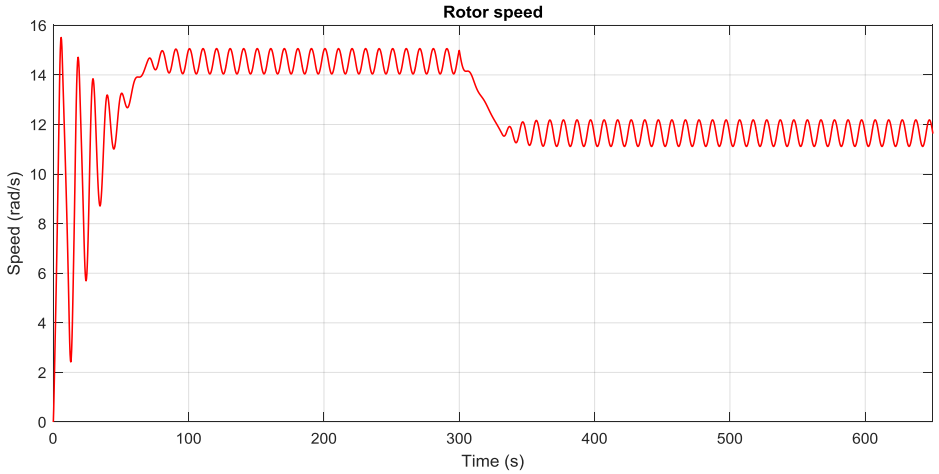

Figure 3.28 The simulated actual rotor speed in rad/s.

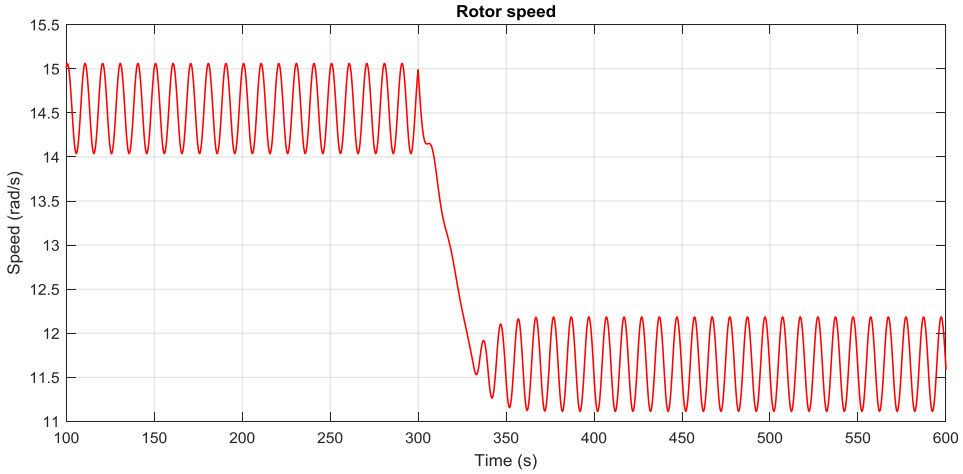

Figure 3.29 The closer view of simulated rotor speed from 100 second to 600 second.

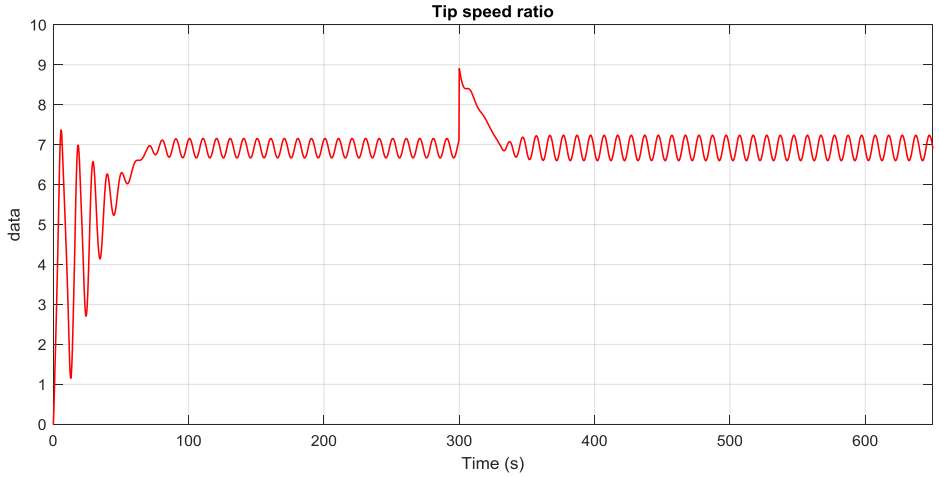

Figure 3.30 The simulated value of the TSR.

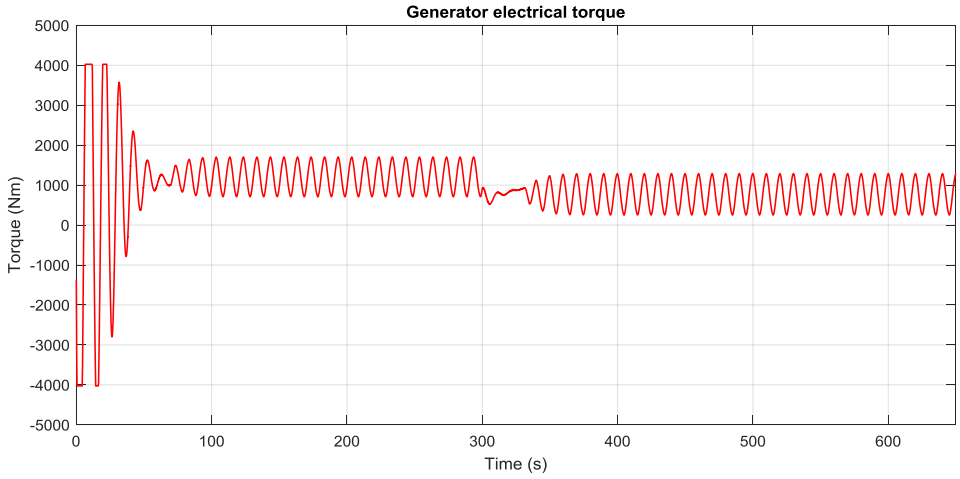

Figure 3.31 The generator torque $\boldsymbol{T_g}$ in Nm.

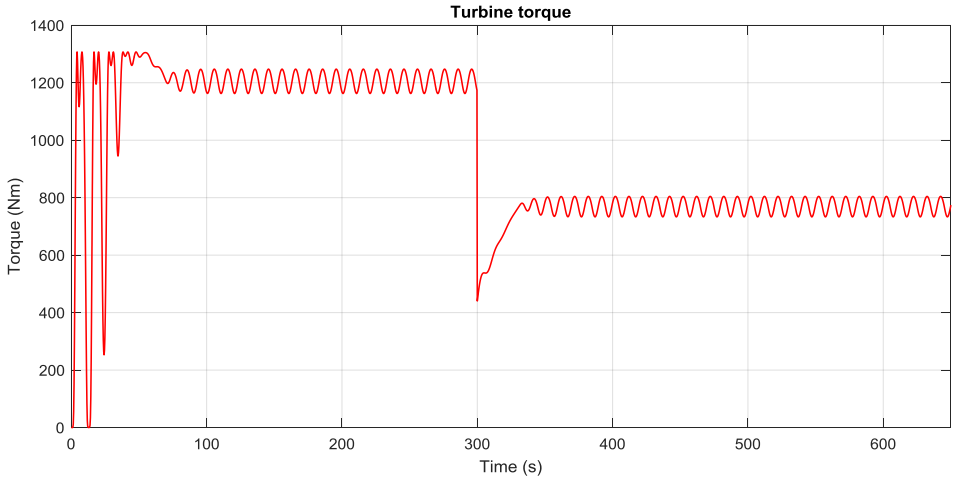

Figure 3.32 The turbine torque $\boldsymbol{T_m}$ in Nm.

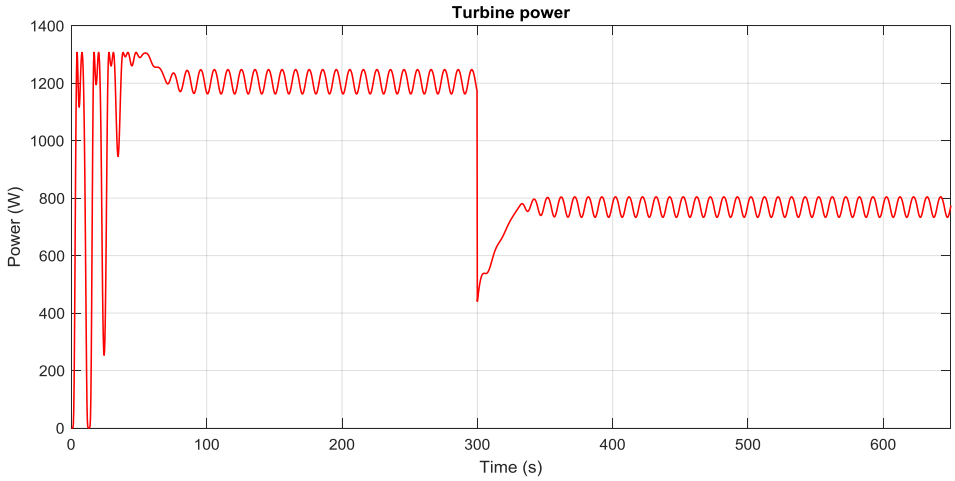

Figure 3.33 Turbine power in Watt.

The following simulation figures from 3.34 to 3.39 are given for the variable wind speed. The wind speeds were measured in every 50 second interval. Since the wind nature is variable so therefore the rotor speed varies according to the wind speed. We see after little transient when both turbine torque and the generator torque are equal, the system reaches to its MPP. Since the algorithm is working with fixed step size there is oscillation around the MPP. In addition, the TSR also reach to the optimum range (6.91) up to 150 second. After that the wind speed is changing gradually upward but due to the inertia of the machine rotor speed becomes stabilized after 250 second. It can be observed very clearly that the rotor speed cannot be changed immediately corresponding to the wind speed variation because of the inertia of the rotor. The same behavior is seen when the wind speed is stable after 400 seconds, the TSR and rotor speed comes in regime after approximately 40 seconds later. The algorithm was created in such a way that if the rotor speed reference becomes below 8 m/s it will hold the previous step of the speed reference. Therefore, when the wind speed drops under 8 m/s the generator will run in the stable speed operation. This phenomenon can be seen from the Figure 3.35.

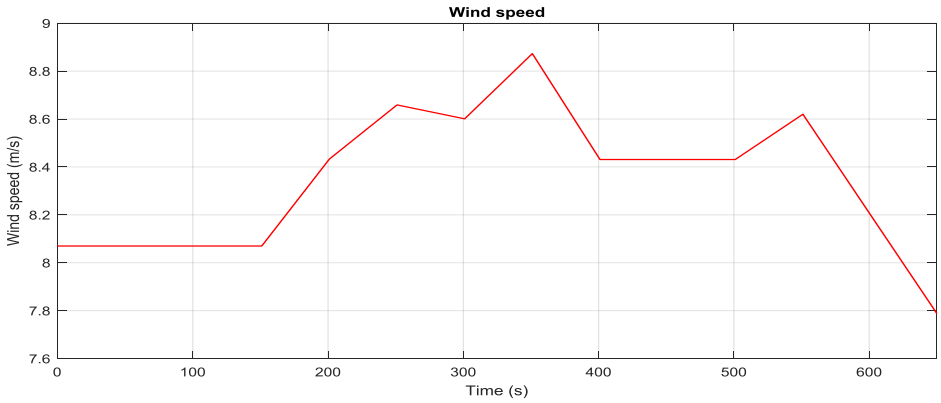

Figure 3.34 Variable wind speed for the HCS control in m/s.

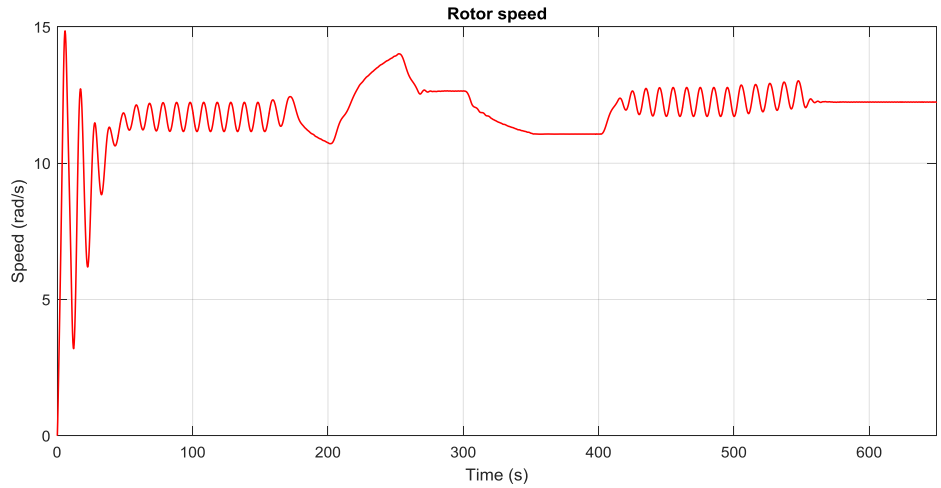

Figure 3.35 Simulated actual rotor speed in rad/s.

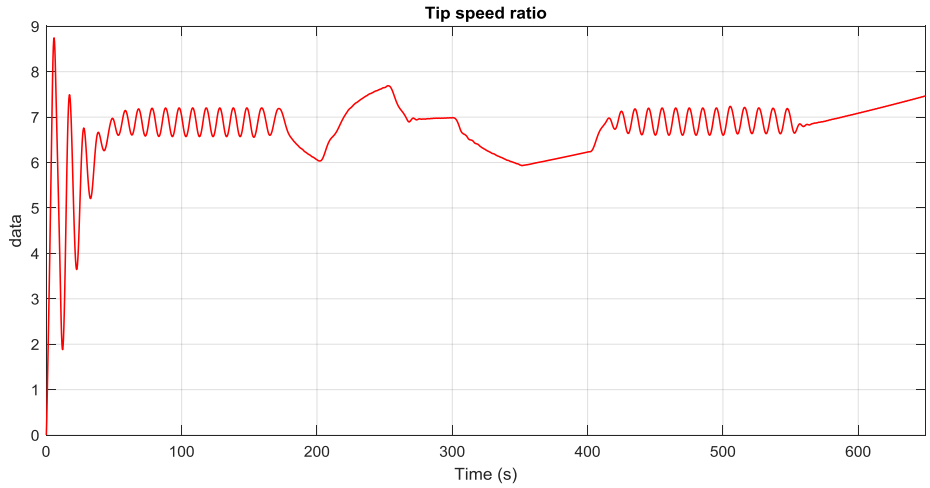

Figure 3.36 Simulated TSR value.

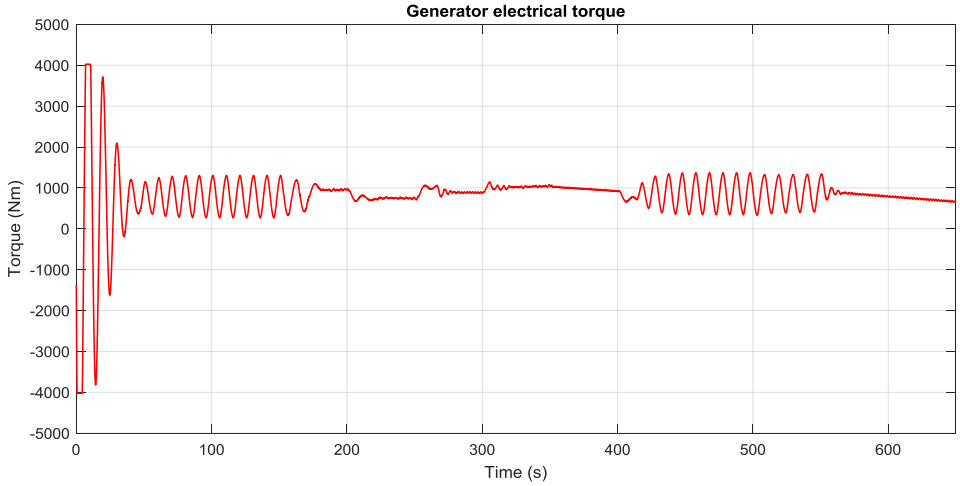

Figure 3.37 Generator torque $\boldsymbol{T_g}$ in Nm.

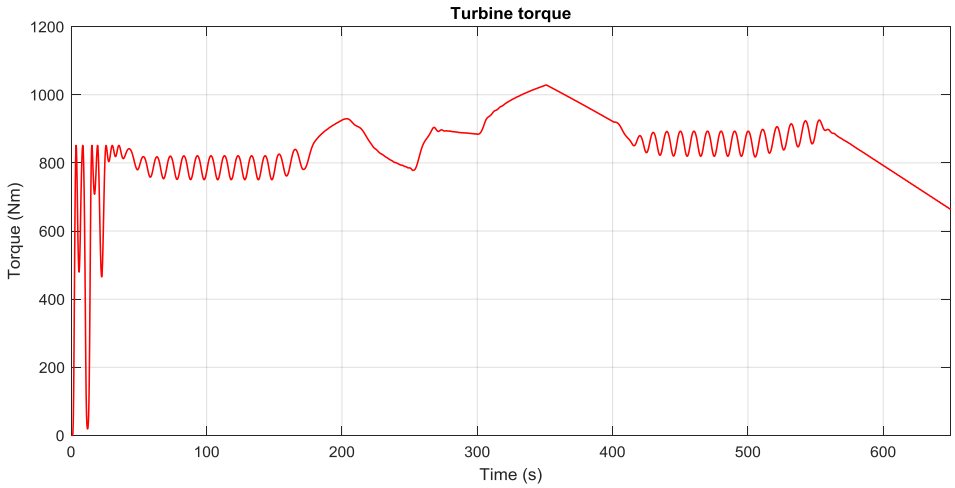

Figure 3.38 Turbine torque in Nm.

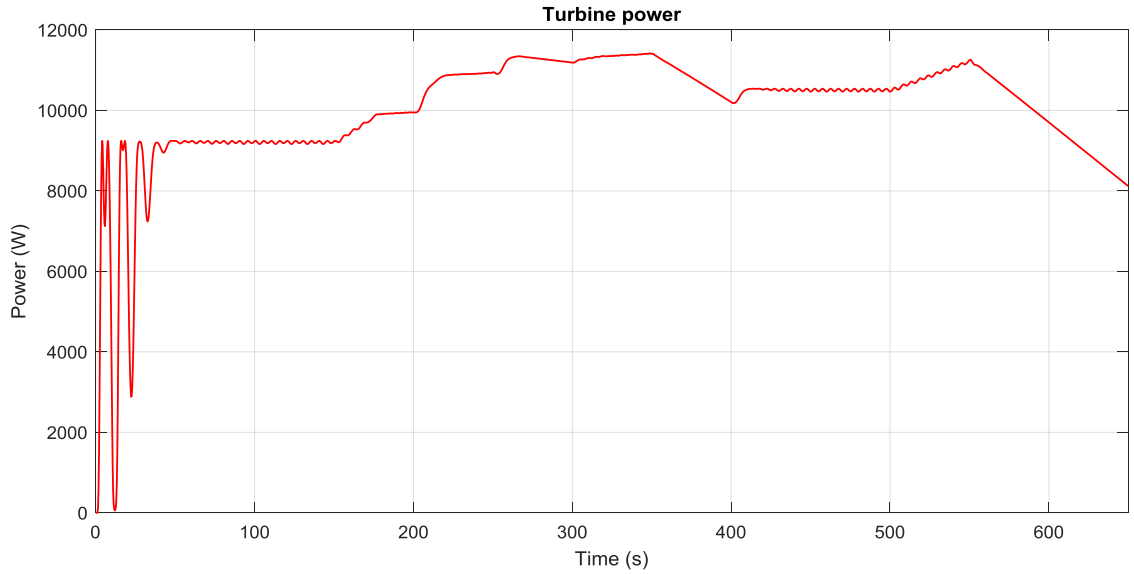

Figure 3.39 Turbine power in Watt.

3.4 Modified hill climb search control

Since the wind speed changes in real scenario, the conventional hill climb search control with fixed step sized rotor speed reference is not well efficient. Furthermore, long settling time is needed for the optimal torque control method for achieving the expected MPP. It was discussed earlier that each control method has its own pros and cons. Therefore, in recent years one new hybrid method was implemented for extracting the MPP where the wind speed measurement and the turbine characteristics are not needed.

The modified hill climb search algorithm is almost similar like HCS control method. The noticeable difference is the MPPT controller uses variable step size for the rotor speed which is a function of the generator speed in the optimal power curve $C_p(\lambda)$ and real generator speed. In this manner the perturbation step size is large at starting when the operating point is far away from the MPP. After that the step size gradually becomes smaller when it arrives near the MPP. The MPPT controller holds the optimal power point at this level since the step size becomes zero until there is a wind speed change. This way we can eliminate the oscillation around the MPP. The new rotor speed reference ($\Delta\omega_{(k)}^{ref}$) is calculated with the following equation

$$\Delta\omega_{(k)}^{ref} = C\frac{dP}{d\omega}, \tag{3.13}$$

where C is a positive constant and the $\frac{dP}{d\omega}$ is the change of turbine power with respect to rotor speed. The value of coefficient C indicates the sensitivity of the variable step speed and it is unitless. At first the earlier rotor speed and the turbine power will be sensed.

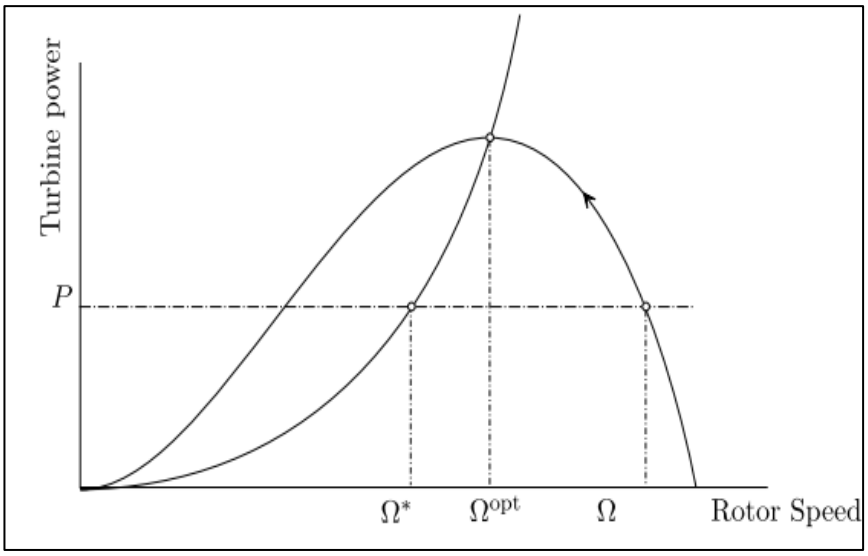

Figure 3.40 The concept of MPPT controller with variable step [1].

After that the following measured rotor speed and the observed power are saved in the MPPT controller memory for determining the next rotor speed step size. The rotor speed with variable step that comes closer to the MPP becomes smaller (see Figure 3.40).

In the figure Ω and P depict the rotor speed and turbine power respectively. A wind speed change is detected if the following conditions are true:

$$\Delta P(k) < 0 \tag{3.14}$$

$$\Delta P(k-1) < 0 \tag{3.15}$$

Likewise, if following conditions are right, wind speed variation can also be sensed.

$$|\omega(k) - \omega(k-1)| \geq A_{threshold} \tag{3.16}$$

$$sign\left(\Delta\omega_{(k)}^{ref}\right) = sign\,\Delta\omega_{(k)} \tag{3.17}$$

In equation $A_{threshold}$ is a small power curve slope threshold.

3.4.1 Simulation model

In the Figure 3.41 the Matlab Simulink model of the modified hill climb search model is presented. The model is basically similar like the previous HCS model except different control algorithm is implemented in the MPPT controller. We see as the inputs it is utilizing the previous rotor speed, the turbine power, the reference rotor speed and time. Eventually the final value of the rotor speed reference is obtained as the output which is later fed in to speed controller. The other outputs are fed back in to the input for generating the new cycle of calculation. The value of the coefficient C for the hill climber was selected 0.001 and it refers the sensitivity of the climber. The value of C was chosen small otherwise for the higher value it will be responsible for creating faster response to the wind speed fluctuation. Note that, if the C value is very large, there will be overshooting specially while the wind speed drops all on a sudden.

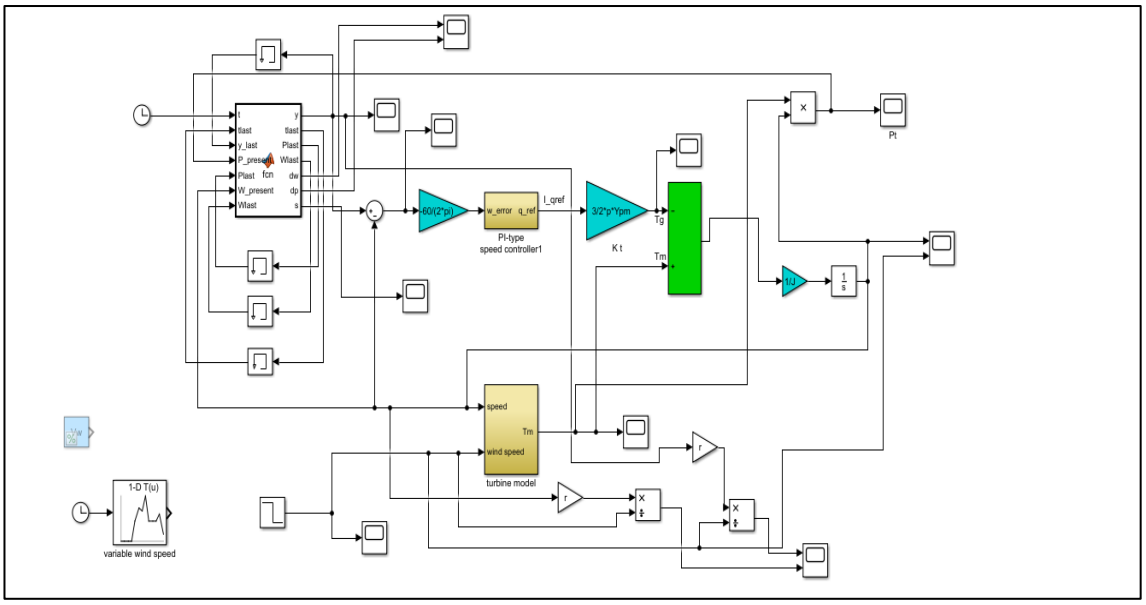

Figure 3.41 Simulink model of modified HCS control.

3.4.2 Simulation results

All the Simulink results with the fixed and variable wind speeds are shown in the following figures. First the control model was tested with the fixed wind speed and the figures from 3.42 to the Figure 3.48 are for the fixed wind speed. Initially when the wind speed was 10 m/s the rotor speed reference step size is estimated based on the slope of the power curve $C_p(\lambda)$. At first, the perturbation size is small (since slope of power curve is small) and gradually it starts to become larger corresponding to slope resulting driving the turbine faster to the MPP. But the more it gets closer to the MPP, the more perturbation size starts to become smaller and eventually the turbine is stabilized in its MPP (slope of power

is zero) until there is wind speed variation (see Figures 3.42, 3.44). Since the control algorithm uses the variable step size therefore the hysteresis is eliminated while the MPP is achieved unlike HCS method. Thus, it is possible to gain zero rotor speed reference step size at MPP. The settling time of the rotor speed is approximately 200 seconds for the initial 10 m/s wind speed which is a slower process comparing to the other control methods. Whenever a step change in the wind speed is applied the rotor starts to follow the wind speed and reaches to its optimal after a certain time. How fast the stable operation will be achieved, it depends on the coefficient C and total system inertia. In the algorithm if the power difference between two cycles is under a specific value (threshold) then it will hold the previous perturbation step size for the next calculation cycle. This is one additional feature to decrease the rotor speed fluctuation like in HCS method. The adaptive memory feature of the modified HCS control method significantly speeds up the MPP tracking. This feature not only allows the algorithms to determine the location of MPP tracked earlier but also enables the method to adapt to any given wind turbine parameters.

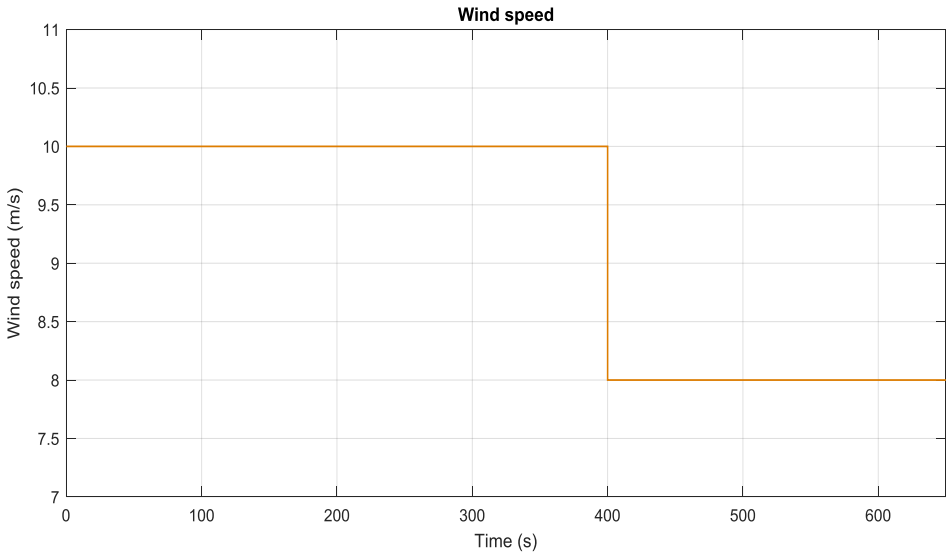

Figure 3.42 Wind speed in m/s.

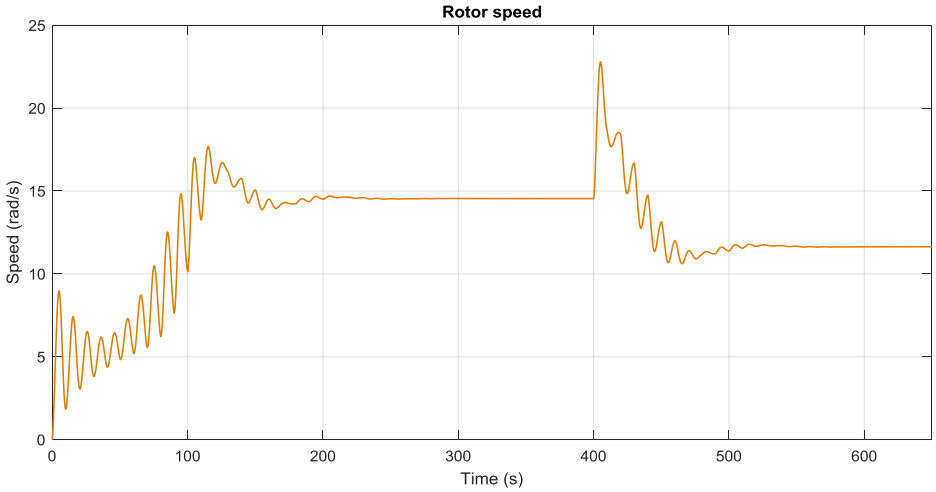

Figure 3.43 Corresponding rotor speed in rad/s.

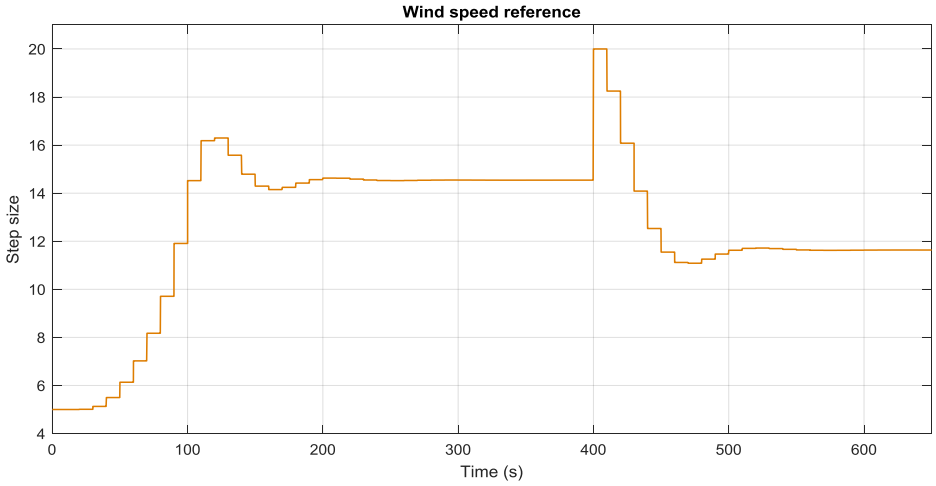

Figure 3.44 Simulated variable rotor speed reference.

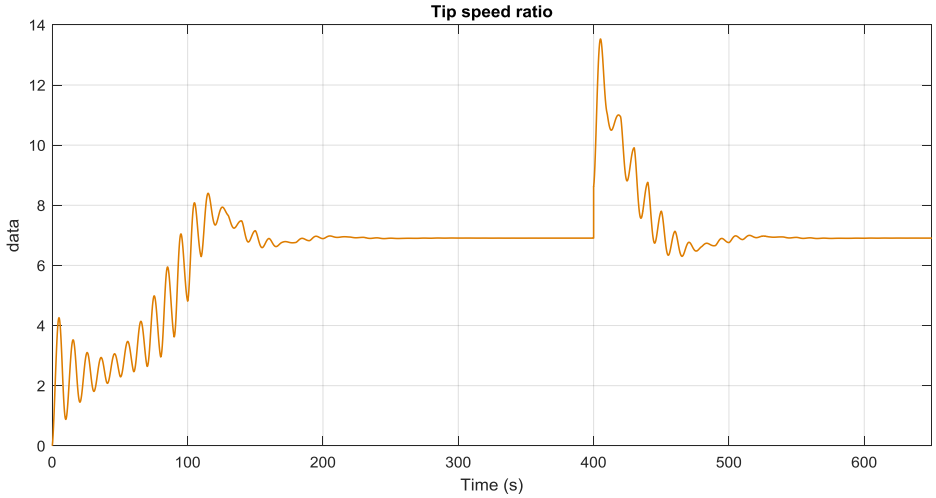

Figure 3.45 Simulated value of TSR.

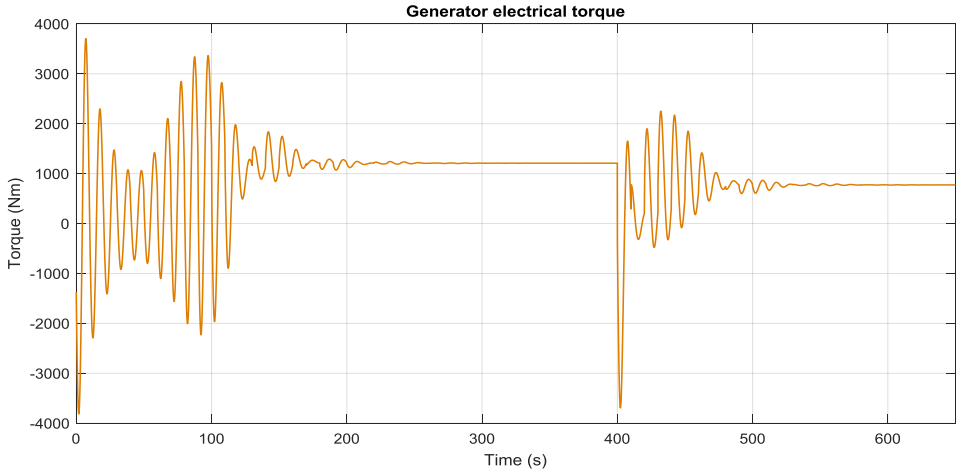

Figure 3.46 Simulated value of generator torque in Nm.

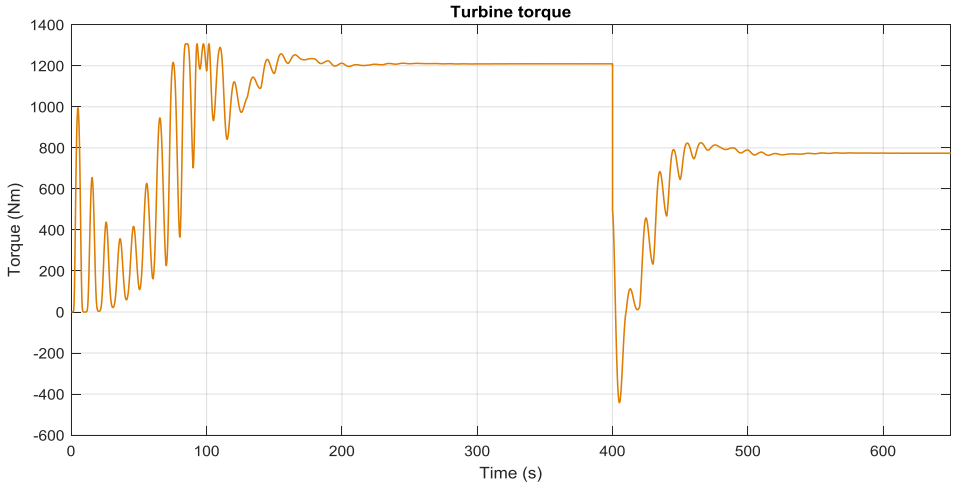

Figure 3.47 Simulated value of turbine torque in Nm.

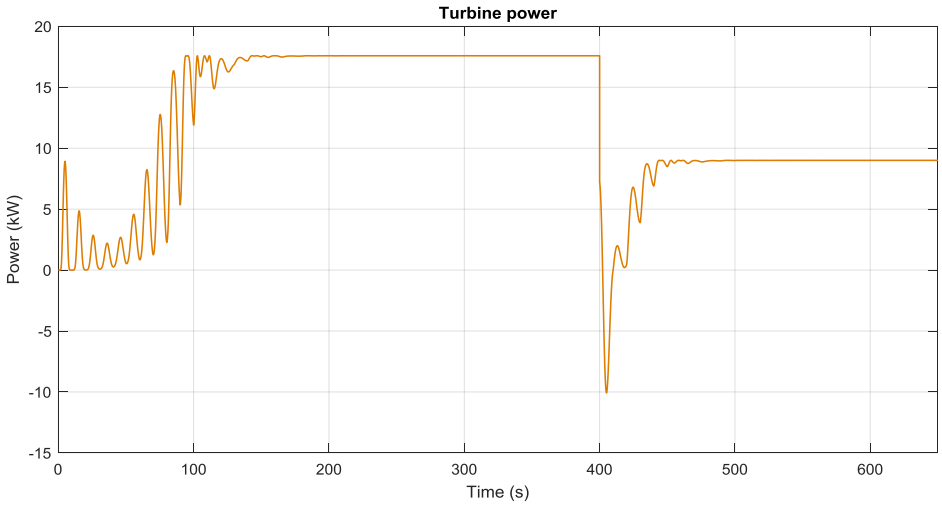

Figure 3.48 Simulated value of turbine power in kW.

After that the variable wind speed is applied for the testing the modified hill climb search method. The Figures from 3.49 to 3.55 are the obtained results from the Simulink. The wind speed varies in a very small limited range which is around 8 m/s to 9 m/s. We see from the Figure 3.50 that the reference speed step size is updated slowly in the beginning of the simulation and approximately after 100 seconds the actual MPP is reached for the initial wind speed of 150 seconds. Next, wind speed is increasing gradually upward but rotor speed follows the wind speed lately. There are two factors which are responsible for affecting the rotor speed slowness i.e. the calculation time of modified HCS and the inertia of the machine. After every time whenever the wind speed is changed, the generator experiences a transient but we cannot utilize the power for calculating the next rotor speed step size during the transient. Therefore, we need to wait for few moments until the system is in regime. This is one reason as well for achieving the MPP and optimum TSR in delay. Overall this control method is efficient and cheaper than the rest of the control methods since we do not need anemometer and wind turbine parameters data. The capability of the control strategy enables the system to extract as much as available power from the fast wind speed variation. The adaptive memory systems of modified HCS gives two types of power managing features.

- Updating the approximate TSR to a magnitude which is closer the actual TSR;
- Saving the determined operating point corresponding to wind speed.

This allows the system to reach the optimal operating point as soon as possible without the time prolonging searching process. The TSR in the Figure 3.52 depicts that approximate TSR is very close to the actual TSR (6.91). For the case when the operating point is not in the ideal value after the determination of the MPP, some small modification is needed to confirm the reliability of the storage data. Therefore, with the little modification minimum power is will be lost during the procedure since the system will be operating very close to the optimal efficiency. It is obvious that the TSR and rotor speed will vary with respect to the wind speed variation but the main purpose of the modified HCS algorithm is to keep the approximate TSR closer to the actual TSR. Therefore, the justification of modified HCS for variable wind speed can be said well efficient since yielding the TSR is nearer to its optimum value.

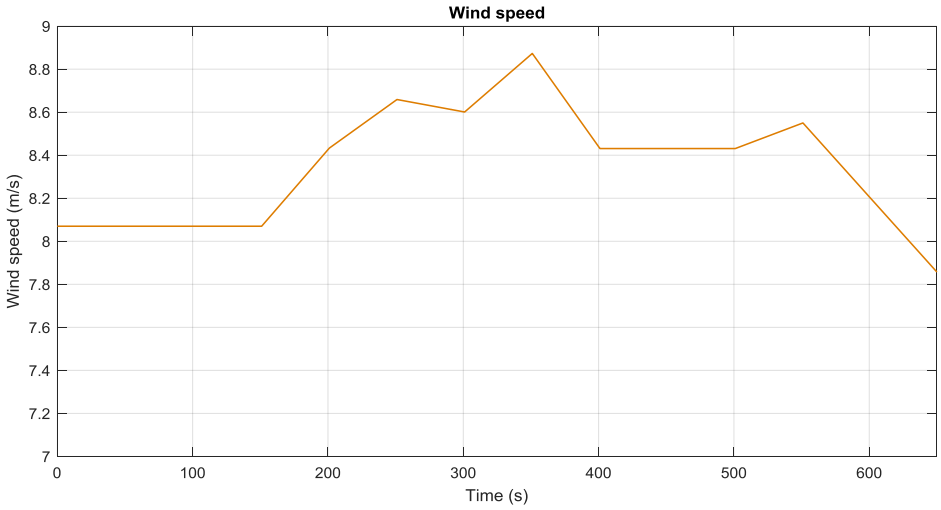

Figure 3.49 Variable wind speed in m/s.

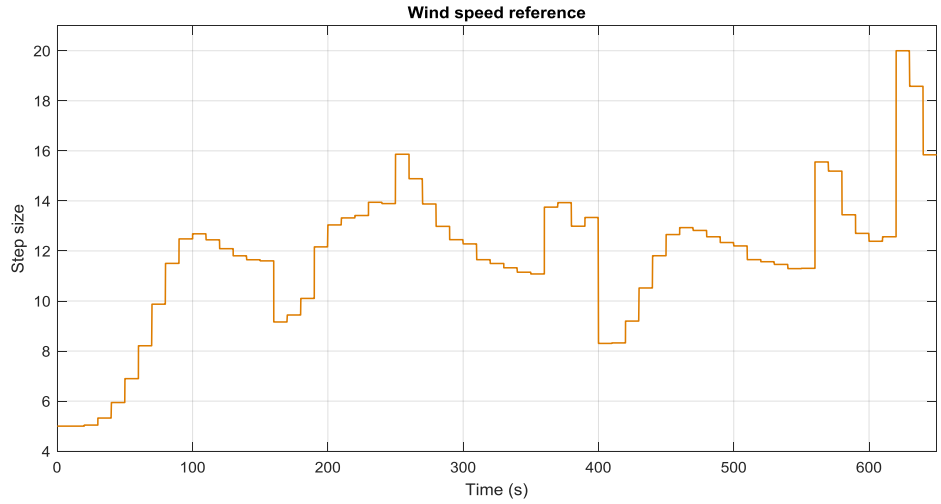

Figure 3.50 Rotor speed reference with variable step.

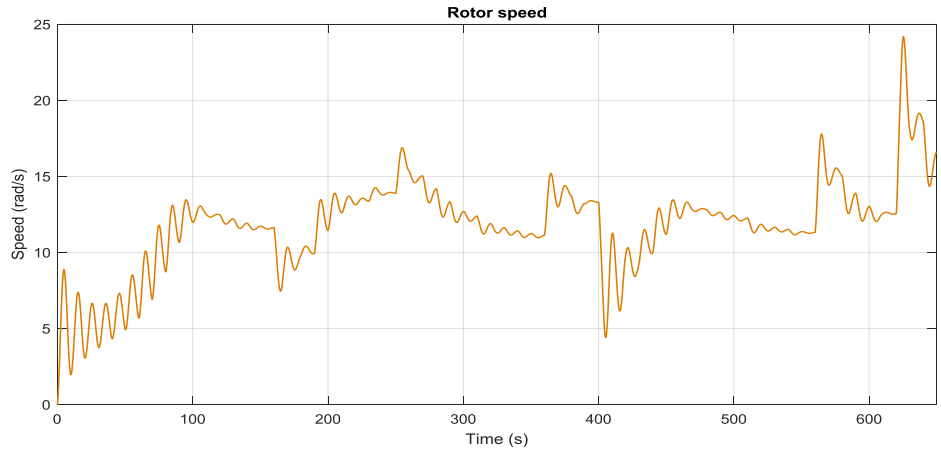

Figure 3.51 Simulated rotor speed in rad/s.

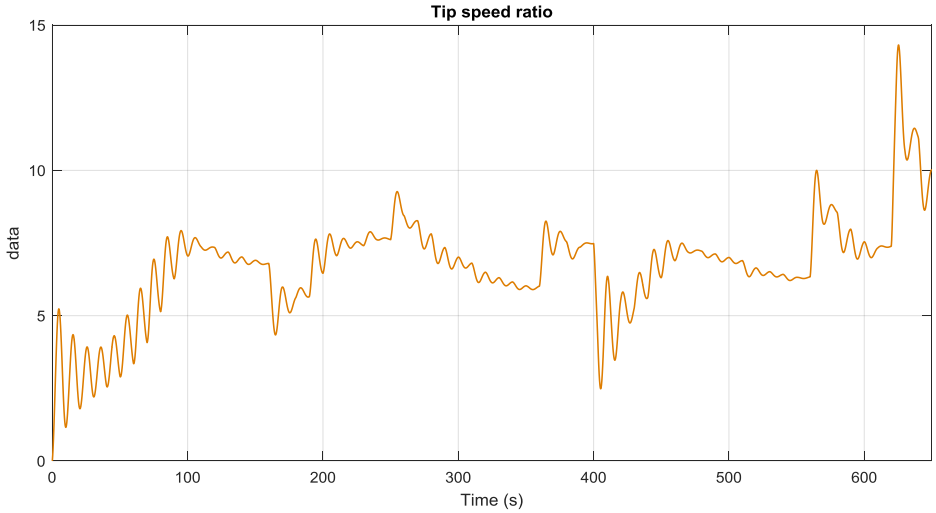

Figure 3.52 Simulated value of TSR.

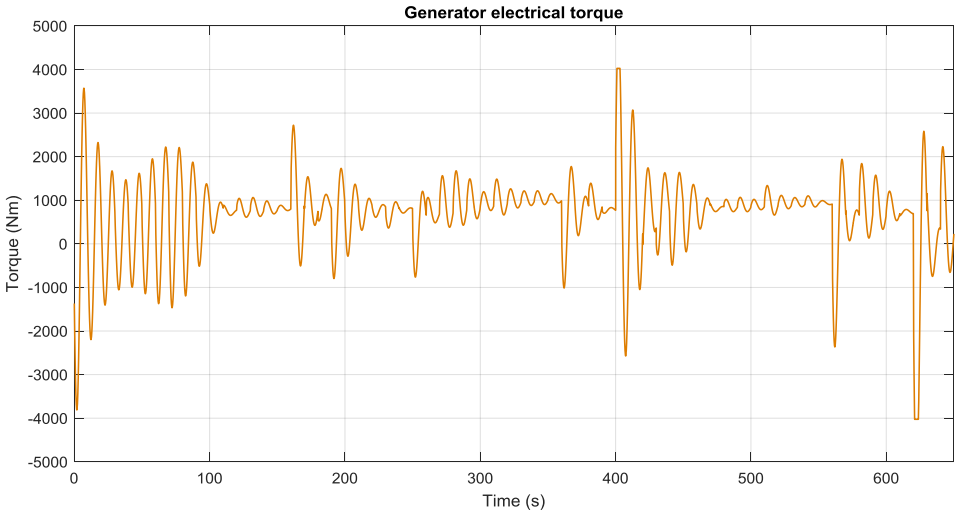

Figure 3.53 Simulated Generator torque in Nm.

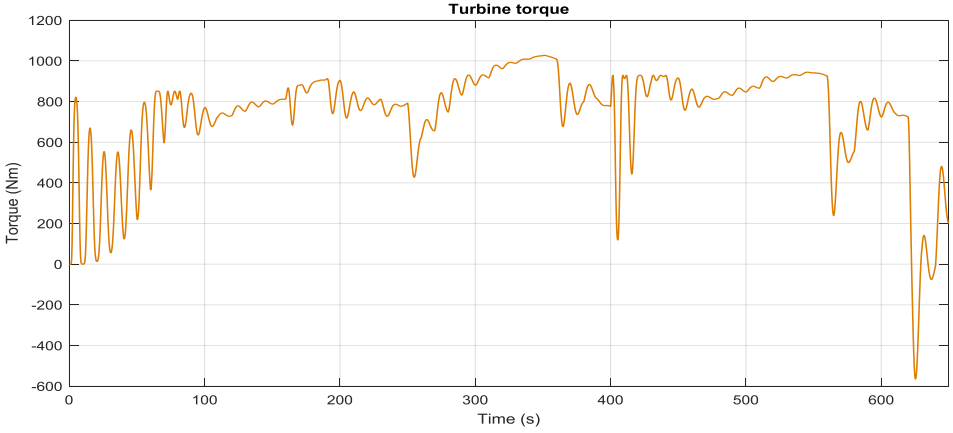

Figure 3.54 Turbine torque value in Nm.

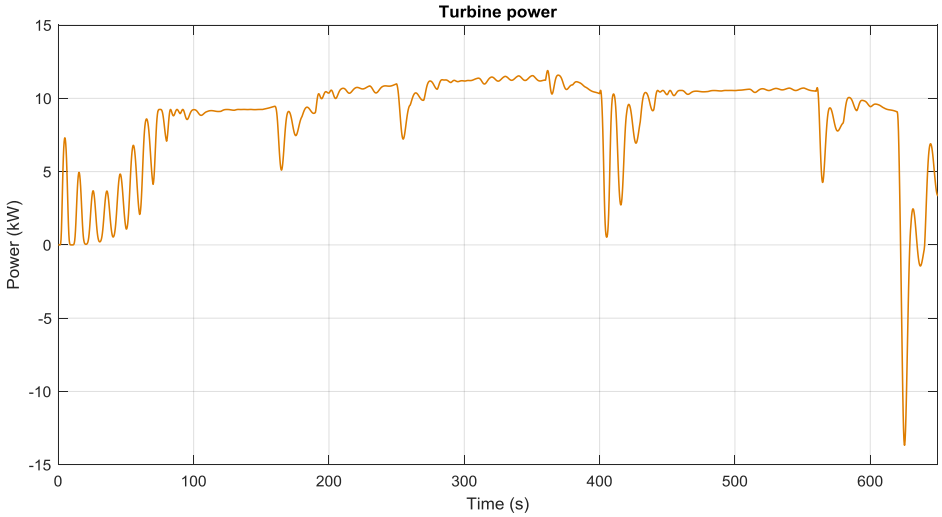

Figure 3.55 Simulated value of turbine power in kW.

4. CONCLUSIONS

In this chapter a conclusion of all the simulated results of the MPPT algorithms will be analyzed based on their efficiency and the related possible future work for further development of the methods such as predictive MPPT.

In chapter 3, four different types of MPPT algorithms are presented with their simulated results. At first, all the theoretical backgrounds are explained and later the ideas are implemented in the Simulink for stable and variable wind speeds. Consequently, the generator rotor speed response and the generator torque responses are observed. In the simulated model, the vector control is supposed to work properly without any type of delay. We observed that the first control method TSR control, controls the turbine to be operating in the optimal tip speed ratio which is obtained from the wind turbine characteristics. This control algorithm is the fastest MPPT solution than others but requires the precise measurement of the wind speed. Hence we need an anemometer or sensor for this measurement. We know that turbines continuously experience wind speed fluctuation at low altitude and sometimes the wind gust as well. Therefore, the proper placement of the anemometer is essential for the accurate wind speed measurement. In the economical point of view this method is not well effective because of the cost of anemometer. Nowadays, in the wind farms classical cup anemometers are installed on the top of the nacelle and behind the rotor. Therefore, because of the presence of blades there is not an accurate measurement of the wind speed. So, it is reasonable to use a correction factor in the algorithm to solve this problem. The requirement for the certain precision of wind speed is a problem for small and medium wind turbines. To increase the reliability different types of sensor technologies are available such as ultrasonic sensors but these are not effective. After all, this TSR control is responsible for determining the precise location of the MPP.

The optimal torque control and hill climb search control do not require any anemometer rather we need to determine the optimal power coefficient value using the machine data sheet and mechanical power. The optimal power coefficient indicates the optimal power of the wind turbine corresponding to the rotor speed. For OTC we do not need any PI controller to generate the reference quadrature axis current. The third control method hill climb search algorithm does not need any prior knowledge of the wind turbine. According to the simulated results we see the settling time for the HCS is longer than the TSR and the OTC methods. Besides, it is not possible to detect the exact location of the MPP and therefore it introduces hysteresis around the actual MPP. This fluctuation of rotor speed is the reason for the poor performance of this control method. The performance of the HCS methods highly depends on the rotor speed reference step size. A higher step size of rotor speed reference accelerates the wind turbine faster towards the MPP but at the same

time larger rotor speed fluctuation can be introduced. On the other hand, with the smaller step size, efficiency of the HCS can be increased but convergence speed of the method will be very slow which is not suitable for the sudden wind speed change. Finally, the fourth method modified hill climb search algorithm allows the hill climber to use the variable step size of the rotor speed reference depending on the region of the $C_p(\lambda)$ curve. With the help of this method the hysteresis of the HCS method can be eliminated as well as the convergence speed can be controlled according to the wind speed variation. In addition, wind speed measurement device such as anemometer is not required for this method but we need PI controller. Overall, the modified hill climb search algorithm is the most efficient control strategy based on the analysis of the simulated results, expenditure and control concept. Furthermore, the system inertia, calculation time of the MPPT controller (hill climber), wind speed characteristics play important role how fast the MPP can be tracked.

The conventional MPPT algorithms are created to follow the wind speed variation. After the detection of the wind speed by the anemometer, the MPPT is executed to detect the new optimal operating point. Basically, the whole procedure is time consuming but for the large wind turbine at high altitude the performance is suitable. However, wind speed changes continuously at low altitude makes the process ineffective. An effective solution could be like placing an anemometer at a specific distance from the wind turbine to estimate the approaching wind speed variation. By this way, the turbine speed could be increased or decreased before a wind speed change reaches at the turbine. The process is called predictive MPPT. The problem arises with this process is that the anemometer gives only the wind speed information from one possible direction. Since the wind has the dominant direction, it is adequate to place anemometer in such a way that it can measure wind speed from only profitable wind direction. In addition, the other solution regarding this problem is several anemometers can be installed in a circular shape. It is obvious to use the cheap anemometers since only the wind speeds need to be measured. In the application of predictive MPPT some factors should be analyzed such as the quantity, proper placement, expected precision of the sensors and the possible increment of the energy harvesting in the MPPT. Furthermore, from the economical point of view the procedure should be optimized for balancing the total cost with energy yield. Eventually, the MPPT scheme should be adapted with the sensor data to control the wind turbine.

REFERENCES

[1] X. Bracke, “Maximum Power Point Tracking of Small Wind Turbines with a Full Active Rectifier,” Master of Science Thesis, Ghent University, Belgium, 2014.

[2] K. Yenduri, P. Sensarma, “Improved maximum power extraction strategy for PMSG based wind energy conversion system,” IET Conference: Power Electronics, Machines and Drives (PEMD), Kanpur, 2012.

[3] S. Morimoto, H. Nakayama, M. Sanada, Y. Takeda, "Sensorless Output Maximization Control for Variable-Speed Wind Generation System Using IPMSG," IEEE Trans. Ind. Appl., Vol. 41, pp. 60.-67, 2005.

[4] Z. Fan, “Mathematical Modelling of Grid Connected Fixed-Pitch Variable-Speed Permanent Magnet Synchronous Generators for Wind Turbines,” Master of Science Thesis, University of Central Lancashire, 2012.

[5] A. Sebaii, M. Hamad, A. Helal, “A sensorless MPPT technique for a grid connected PMSG wind turbine system,” Journal of Renewable Power Generation, Vol. 6, No. 1, 2013.

[6] Z. Dalala, Z. Zahid, W. Yu, Y. Cho, J. Lai, “Design and Analysis of an MPPT Technique for Small-Scale Wind Energy Conversion Systems,” Vol. 28, No. 1, IEEE Trans. Energy Conv., 2013.

[7] K. Vigneswaran, Dr P. Kumar, “Maximum Power Point Tracking (MPPT) Method in Wind Power System,” International Journal of Innovative Research in Science, Engineering & Technology, Vol. 28, 2016.

[8] M. Abdullah, A. Yatim, C. Wei, Tan, “A Study of Maximum Power Point Tracking Algorithms for Wind Energy Systems,” IEEE First Conference on Clean Energy and Technology CET, 2011.

[9] C. Ghiţă1, A. Chirilă1, D. Deaconu1, D. Ilina, “Wind turbine permanent magnet synchronous generator magnetic field study,” University Politehnica of Bucharest, Splaiul Independenţei, Bucharest, 2016.

[10] W. Cao, Y. Xie, Zheng Tan, “Wind Turbine Generator Technologies,” Chapter 7, University of Newcastle Upon Tyne, United Kingdom; Harbin University of Science and Technology, P. R. China, 2012.

[11] E. Hamatwi, M. Gitau, E. Davidson, " Control of a Direct-driven Permanent Magnet Synchronous Generator-based Wind Turbine to Achieve Maximum Wind-Power Extraction," IEEE PES-IAS Power Africa, Ghana, 2017.

[12] L. Deisadze, D. Digeser, C. Dunn, D. Shoikat, "Vertical Axis Wind Turbine Evaluation and Design," Worcester Polytechnic Institute, 2013.

[13] J. De Kooning, "Optimal Current Waveform Shaping and Intelligent Maximum Power Point Tracking for Wind Turbines," Dissertation, Ghent University, Faculty of Engineering and Architecture, 2015.

[14] J. Sarkar, Prof. Shridhar, S. Khule, "A Study of MPPT Schemes in PMSG Based Wind Turbine System," International Conference on Electrical, Electronics and Optimization Techniques (ICEEOT), 2016.

[15] M. Uddin, N. Patel, "Maximum Power Point Tracking Control of IPMSG Incorporating Loss Minimization and Speed Sensorless Schemes for Wind Energy System," IEEE Trans. Ind. Appl., Vol. 52, 2015.

[16] B. Akin, M. Bhardwaj, "Field Orientated Control of 3-Phase AC-Motors," Texas Instruments Europe, Literature Number: BPRA073, 1998.

[17] V. Erling, "Implementation of Interior Permanent Magnet Synchronous Machines and Control in a Wind Power Emulating Test Bench," Master of Science Thesis, Tampere University of Technology, 2017.

[18] M. Li, J. He, N. Demerdash, "Flux-Weakening Control for Permanent-Magnet Synchronous Motors Based on Z-Source Inverters," Transportation Electrification Conference and Expo, 2014.

[19] H. Jeong, R. Seung, K. Lee, "An Improved Maximum Power Point Tracking Method for Wind Power Systems, Energies, Vol. 5, 2012.

[20] M. Nodoushan, M. Akhbari, "Optimal Torque Control of PMSG-based Stand-Alone Wind Turbine with Energy Storage System," Journal of Electric Power & Energy Conversion Systems," Vol. 1, pp. 52.-59, 2016.

[21] P. Shukla, N. Tiwari, S.L, "Maximum Power Point Tracking Control for Wind Energy Conversion System," A Review. International Journal of Advanced Research in Electrical, Electronics and Instrumentation Engineering, Vol. 4, 2015.

[22] M. Gómez, E. Ribeiro, J. Estima, C. Boccaletti, A. Cardoso, "Development of an Effective MPPT Method Suitable to a Stand-Alone, Low-Cost Wind Turbine System," Industrial Electronics Society, IECON, 2016.

[23] Y. Zhu, M. Cheng , W. Hua, Wei Wang, “A Novel Maximum Power Point Tracking Control for Permanent Magnet Direct Drive Wind Energy Conversion Systems,” Energies, Vol. 5, No. 5, pp.1398-1412, 2012.

[24] L. Li, B. Han, Y. Ren, J. Brindley, L. Jiang, “An Improved Hybrid Hill Climb Searching Control for MPPT of Wind Power Generation Systems under Fast Varying Wind Speed,” International Conference on Renewable Power Generation, pp. 1-6, 2015.

APPENDIX A: MACHINE DATA SHEETS

Electrical characteristics of motor and generator

	Motor	Generator
Power	17 kW	13.5 kW
Voltage	370 V	370 V
Frequency	12.7 Hz	12.7 Hz
Speed	127 rpm	127 rpm
Current	34 A	33.1 A
Power Factor	0.96	0.65
Torque	1279 Nm	1016 Nm
Number of Poles	6	6

Equivalent circuit characteristics in star connection

	Motor	Generator
Stator resistance	700 mΩ	700 mΩ
d-axis inductance	56 mH	56 mH
q-axis inductance	71 mH	71 mH
Permanent magnet flux linkage	3.1851 Wb	3.1851 Wb